Journal of Engineering Mechanics

Vibration attenuations and amplifications of one-dimensional uncoupled and coupled systems with optimal metafoundations

--Manuscript Draft--

Manuscript Number:	EMENG-5178R1
Full Title:	Vibration attenuations and amplifications of one-dimensional uncoupled and coupled systems with optimal metafoundations
Manuscript Region of Origin:	CHINA
Article Type:	Technical Paper
Funding Information:	National Natural Science Foundation of China (CN) (51778488) — Dr Fei Sun Horizon 2020 (730900) — Oreste Salvatore Bursi
Abstract:	Finite locally resonant metafoundations represent an innovative solution for structural seismic response mitigation based on their filtering capabilities at selected frequency ranges. They inherit the filtering properties of periodic foundations and bands in which response amplitudes are reduced, the so-called attenuation zones. Nonetheless, other bands of vibration-induced resonances amplify the components of superstructure response and are generally named non-attenuation zones. Both frequency bandwidths and amplifications depend on the dynamic properties of metafoundations and superstructures as well as their coupling. Thus, in order to shed light on the mechanisms of seismic mitigation of coupled systems endowed with optimal metafoundations, this paper explores both elastic uncoupled and coupled unit-cell chains in the frequency domain based on the analysis of various transfer functions. Moreover, to address uncertainty at the excitation level, time history analyses are carried out with a set of natural accelerograms that characterize operating basis earthquakes; thus, response contributions from both attenuation zones and non-attenuation zones can be distinguished by relating response variances to peak responses. Eventually, the attenuation effects of optimal metafoundations, the frequency shift of superstructures due to unit cells of metafoundations and the coupling of both attenuation zones and non-attenuation zones are analyzed in depth.
Corresponding Author:	Fei-fei Sun Tongji University Shanghai, Shanghai CHINA
Corresponding Author E-Mail:	ffsun@tongji.edu.cn
Order of Authors:	Lei Xiao Fei Sun Oreste Salvatore Bursi
Suggested Reviewers:	
Opposed Reviewers:	
Additional Information:	
Question	**Response**
Authors are required to attain permission to re-use content, figures, tables, charts, maps, and photographs for which the authors do not hold copyright. Figures created by the authors but previously published under copyright elsewhere may require permission. For more information see	No

http://ascelibrary.org/doi/abs/10.1061/9780784479018.ch03. All permissions must be uploaded as a permission file in PDF format. Are there any required permissions that have not yet been secured? If yes, please explain in the comment box.	
ASCE does not review manuscripts that are being considered elsewhere to include other ASCE Journals and all conference proceedings. Is the article or parts of it being considered for any other publication? If your answer is yes, please explain in the comments box below.	No
Each submission to ASCE must stand on its own and represent significant new information, which may include disproving the work of others. While it is acceptable to build upon one's own work or replicate other's work, it is not appropriate to fragment the research to maximize the number of manuscripts or to submit papers that represent very small incremental changes. ASCE may use tools such as CrossCheck, Duplicate Submission Checks, and Google Scholar to verify that submissions are novel. Does the manuscript constitute incremental work (i.e. restating raw data, models, or conclusions from a previously published study)?	No
Authors are expected to present their papers within the page limitations described in <u><i>Publishing in ASCE Journals: A Guide for Authors</u></i>. Technical papers and Case Studies must not exceed 30 double-spaced manuscript pages, including all figures and tables. Technical notes must not exceed 7 double-spaced manuscript pages. Papers that exceed the limits must be justified. Grossly over-length papers may be returned without review. Does this paper exceed the ASCE length limitations? If yes, please provide justification in the comments box below.	No
All authors listed on the manuscript must have contributed to the study and must approve the current version of the manuscript. Are there any authors on the paper that do not meet these criteria? If	No

the answer is yes, please explain in the comments.	
Was this paper previously declined or withdrawn from this or another ASCE journal? If so, please provide the previous manuscript number and explain what you have changed in this current version in the comments box below. You may upload a separate response to reviewers if your comments are extensive.	Yes
Please provide the previous manuscript number and explain what you have changed in this current version in the comments box below. You may upload a separate response to reviewers if your comments are extensive. as follow-up to "Was this paper previously declined or withdrawn from this or another ASCE journal? If so, please provide the previous manuscript number and explain what you have changed in this current version in the comments box below. You may upload a separate response to reviewers if your comments are extensive. "	This manuscript is a revised version of a previous manuscript, “Evaluation and control of coupling behavior between attenuation and non-attenuation zones in finite locally resonant acoustic metamaterials for low frequencies”. Manuscript Number: EMENG-4542. Thanks to the comments of the two Reviewers, we have rearranged our article to make motivations and concepts clear. The main changes in the paper are listed herein. Research object In the revised version, we focus on locally resonant metafoundations (MFs). We agree with Reviewer #1 that a 1D mass-in-mass model is not suitable to simulate metabarriers, and the amplification phenomenon does not happen in metabarriers. We think the 1D mass-in-mass model is capable of simulating major characteristics of MFs and the amplification phenomenon can be important in the use of MFs not properly designed. Detailed explanations are given in response to specific comments. Research objective The research objective of the previous manuscript intended to illustrate the coupling effect of attenuation and non-attenuation zones (AZ and NAZ) on the mitigation effect of a metafoundation in an uncoupled system. However, the uncoupled system is an approximation of the coupled system. In actual engineering, a superstructure is connected to a metafoundation, which represents a coupled system. In the revised version, besides the interaction of the two zones, the research objective is to explain the performance of MFs in both an uncoupled and coupled system. Research methods Several methods in the previous manuscript have been removed, including artificial modification of the Fourier amplitudes of the frequency components, employment of a β factor to estimate the response attenuation due to the AZ, and the concept of “ideally filtered wave”. In the revised paper, the work is based on the frequency transfer function, and most of the work is based on the Transfer-Matrix method. Nevertheless, to illustrate the contribution of each mode and the cause of amplification, the modal superposition method is employed in Subsection “Amplification in NAZs”. Two types of systems are investigated: the uncoupled and coupled systems, respectively. The uncoupled system helps illustrate the coupling effect between AZ and NAZ, and also the frequency shift of superstructure due to unit cells, both of which play a role in mitigation effect of PFs in the coupled system. To achieve a favorable mitigation effect, metafoundations in different systems are first optimized. Parameters of metafoundations The parameters used for the metafoundations in the previous manuscript were general. In the revised paper, initial parameters are taken from the work of Basone et al. [1]. Earthquake accelerograms In the previous manuscript, we used the accelerogram sets of FEMA P695. In the revised paper, in order to optimize the massive resonators of MFs, the set of

	accelerograms corresponding to operating basis earthquakes (OBE) with a 10% probability of exceedance in 50 years is adopted. Nonetheless, to avoid damage, the MFs have been designed with safe shutdown earthquakes (SSE) with 2% probability of exceedance in 50 years. The average power spectral density (PSD) of the accelerograms is fitted with the Kanai-Tajimi filter modified by Clough and Penzien (denoted as KC filter). The KC-fitted PSD is then adopted to optimize metafoundations in the frequency domain. The aforementioned accelerograms are employed to verify the optimized metafoundations in the time domain.
Companion manuscripts are discouraged as all papers published must be able to stand on their own. Justification must be provided to the editor if an author feels as though the work must be presented in two parts and published simultaneously. There is no guarantee that companions will be reviewed by the same reviewers, which complicates the review process, increases the risk for rejection and potentially lengthens the review time. If this is a companion paper, please indicate the part number and provide the title, authors and manuscript number (if available) for the companion papers along with your detailed justification for the editor in the comments box below. If there is no justification provided, or if there is insufficient justification, the papers will be returned without review.	
If this manuscript is intended as part of a Special Issue or Collection, please provide the Special Collection title and name of the guest editor in the comments box below.	
Recognizing that science and engineering are best served when data aremade available during the review and discussion of manuscripts andjournal articles, and to allow others to replicate and build on workpublished in ASCE journals, all reasonable requests by reviewers formaterials, data, and associated protocols must be fulfilled. If you are restricted from sharing your data and materials, please explain below.	
Papers published in ASCE Journals must make a contribution to the core body of knowledge and to the advancement of the field. Authors must consider how their new knowledge and/or innovations add value to the state of the art and/or state of	(1)The seismic mitigation performance of metafoundation in coupled systems are understood through the comparison of the coupled and uncoupled systems. It is a combination of base-isolation effects, a wider attenuation zone due to coupling and the best balance between attenuation zones (AZs) and non-attenuation zones (NAZs). (2)Both the response contributions of AZs and NAZs can be distinguished by relating response variances and peak responses. It is proved that the contribution from NAZs

the practice. Please outline the specific contributions of this research in the comments box.	metters in seismic mitigation effect of metafoundations, which is typically neglected but must be kept in mind when designing metamaterials for seismic mitigation.
The flat fee for including color figures in print is $800, regardless of the number of color figures. There is no fee for online only color figures. If you decide to not print figures in color, please ensure that the color figures will also make sense when printed in black-and-white, and remove any reference to color in the text. Only one file is accepted for each figure. Do you intend to pay to include color figures in print? If yes, please indicate which figures in the comments box.	No
Is this article or parts of it already published in print or online in any language? ASCE does not review content already published (see next questions for conference papers and posted theses/dissertations). If your answer is yes, please explain in the comments box below.	No
Has this paper or parts of it been published as a conference proceeding? A conference proceeding may be reviewed for publication only if it has been significantly revised and contains 50% new content. Any content overlap should be reworded and/or properly referenced. If your answer is yes, please explain in the comments box below and be prepared to provide the conference paper.	No
ASCE allows submissions of papers that are based on theses and dissertations so long as the paper has been modified to fit the journal page limits, format, and tailored for the audience. ASCE will consider such papers even if the thesis or dissertation has been posted online provided that the degree-granting institution requires that the thesis or dissertation be posted. Is this paper a derivative of a thesis or dissertation posted or about to be posted on the Internet? If yes, please provide the URL or DOI permalink in the comment box below.	No
If there is anything else you wish to	

communicate to the editor of the journal, please do so in this box.	
When submitting a new and revised manuscript, authors are asked to include a Data Availability Statement containing one or more of the following statements, with specific items listed as appropriate. Please select any of the statements below that apply to your manuscript. Also, please include the selected statements in a separate "Data Availability Statement" section in your manuscript, directly before the acknowledgements or references.	c. Some or all data, models, or code that support the findings of this study are available from the corresponding author upon reasonable request.

Vibration attenuations and amplifications of one-dimensional uncoupled and coupled systems with optimal metafoundations

Lei Xiao, Feifei Sun, Oreste Salvatore Bursi

Lei Xiao
College of Civil Engineering, Tongji University, 1239 Siping Road, Shanghai 200092, China
1410213@tongji.edu.cn

Feifei Sun
Corresponding author
Professor
State Key Laboratory of Disaster Reduction in Civil Engineering, Tongji University, 1239 Siping Road, Shanghai 200092, China
ffsun@tongji.edu.cn

Oreste Salvatore Bursi
Professor
Department of Civil, Environmental and Mechanical Engineering, University of Trento, Via Mesiano, 77, 38123 Trento, Italy
Oreste.Bursi@unitn.it

Abstract

Finite locally resonant metafoundations represent an innovative solution for structural seismic response mitigation based on their filtering capabilities at selected frequency ranges. They inherit the filtering properties of periodic foundations and bands in which response amplitudes are reduced, the so-called attenuation zones. Nonetheless, other bands of vibration-induced resonances amplify the components of superstructure response and are generally named non-attenuation zones. Both frequency bandwidths and amplifications depend on the dynamic properties of metafoundations and superstructures as well as their coupling. Thus, in order to shed light on the mechanisms of seismic mitigation of coupled systems endowed with optimal metafoundations, this paper explores both elastic uncoupled and coupled unit-cell chains in the frequency domain based on the analysis of various transfer functions. Moreover, to address uncertainty at the excitation level, time history analyses are carried out with a set of natural accelerograms that characterize operating basis earthquakes; thus, response contributions from both attenuation zones and non-attenuation zones can be distinguished by relating response variances to peak responses. Eventually, the attenuation effects of optimal metafoundations, the frequency shift of superstructures due to unit cells of metafoundations and the coupling of both attenuation zones and non-attenuation zones are analyzed in depth.

Author keywords Finite locally resonant metafoundation; Coupled and uncoupled system; Attenuation zone; Non-attenuation zone

Introduction

Background and motivation

Recently, periodic materials have received growing interest in material and structures due to their ability to provide high attenuation in selective frequency ranges; these frequency ranges are called stop bands. The frequency bands other than the stop bands are identified as pass bands wherein the waves are transmitted without any attenuation. To date, there are mainly two types of periodic materials: phononic crystals and locally resonant metamaterials (Hussein et al., 2014). Locally resonant metamaterials are better suited for attenuation of low-frequency vibrations due to their ability to form stop bands associated with massive inner resonators that entail local antiresonances (Liu et al., 2000; Wang et al., 2014; Basone et al., 2018). Therefore, the band-pass property of locally resonant metamaterials opens an innovative direction towards structural seismic protection (Achaoui et al., 2015; Finocchio et al., 2014; Miniaci et al., 2016).

To crystallize the ideas, two types of applications have been proposed: i) metabarriers to redirect surface waves back into the ground (Dertimanis et al., 2016; Kim and Das, 2012; Krödel et al., 2015; Geng et al., 2018; Wagner et al., 2018); and ii) metafoundations to counteract the effects of seismic waves (La Salandra et al., 2017; Cheng and Shi, 2018a; Huang et al., 2017; Cheng and Shi, 2013; Bao et al., 2012). More precisely, in order to mitigate surface waves, barriers were proposed to be buried around the target building; along this line, to show the practical feasibility of a seismic metabarrier, a large scale *in situ* experiment was carried out by Brûlé et. al (Brûlé et al., 2014). Furthermore, Palermo et. al. investigated a conversion mechanism on surface waves both with FE analyses and a scaled experiment (Palermo et al., 2016; Palermo et al., 2018). The feasibility of forests as seismic metabarriers was demonstrated by geophysical tests and FE analyses carried out by Colombi et al. (Colombi et al., 2016a; Colombi et al., 2016b). Conversely, in order to mitigate seismic waves, metafoundations can be placed beneath a superstructure. In this respect, numerous configurations of composite cells have been conceived (Cheng and Shi, 2013; Cheng and Shi, 2018b; Casablanca et al., 2018). In particular, Basone et al. (2018) proposed a novel metafoundation composed of unit cells made of flexible shear frames to entail base-isolation effects and massive resonators to generate wide AZs. The effectiveness of one-dimensional (1D) (Xiang et al., 2012), two-dimensional (2D) (Yan et al., 2014) and three-dimensional (3D) (Yan et al., 2015) locally resonant metafoundations have been experimentally verified on scaled models. Of particular interest for the present work is the concept of finite locally resonant metafoundations, the so-called MFs.

In order to conceive and analyze an MF subjected to seismic records, two approaches can be used. The first one considers the MF and the superstructure as an uncoupled system; and the response at the top of the MF, i.e., at Point #1 of Fig. 1(a), is defined as a filtered accelerogram that represents the excitation for the superstructure (Cheng and Shi, 2013; Cheng and Shi, 2018b; Yan et al., 2015; Yan et al., 2014; Xiang et al., 2012; Casablanca et al., 2018). With this assumption, one designs a MF that exhibits an AZ covering the main eigenfrequencies of the superstructure, namely those frequency components which contribute most to the superstructure response. Nonetheless, this approach neglects possible response amplifications in the non-attenuation zone (NAZ) and the frequency shift of the superstructure due to its interaction with the MF. More precisely, MFs may entail additional response resonant peaks in NAZ (Geng et al., 2018; Cheng and Shi, 2018b; Yan et al., 2014; Yan et al., 2015). As a result, the actual mitigation effect of an MF depends on whether the attenuation obtained in the AZ will prevail on amplification effects in the NAZ. Besides, when a superstructure is connected to a flexible MF, the coupled eigenfrequency shifts to a lower value (Basone et al., 2018). Therefore, the AZ previously designed may fail to cover the new eigenfrequency.

The second approach is more accurate and considers both the MF and the superstructure as a coupled system (Basone et al., 2018); see Fig. 1(c). As a result, the coupled system can properly take into account the aforementioned interaction effects. Nonetheless, mitigation effects on the superstructure response are not explored in depth; in particular, they depend on base-isolation effects entailed by finite unit cells, the frequency range of AZs and resulting NAZs, indeed.

Scope

In order to shed light on both mechanisms and performance of MFs, especially the coupling effect of AZs and NAZs, this article proposes a phased approach which relies on the analysis of both uncoupled and coupled systems. More precisely, this research work is a continuation of the work by Basone et al. (Basone et al., 2018). Therefore, we start with the MF designed and optimized to control the response of a slender tank subjected to site-specific ground motion spectra, and we consider the main dynamic properties of the relevant superstructure. Herein, the MF is optimized in both uncoupled and coupled system configuration, respectively. Successively, to illustrate the influence of the superstructure frequency shift and the coupling effect between AZs and NAZs, the performance of an MF in an uncoupled system is investigated in depth. As a result, the role of an MF and its effect in both uncoupled and coupled systems are understood. The remainder of the paper is organized as follows. The paper introduces the system of equations of motion for different uncoupled and coupled systems. Successively, a suitable optimization procedure is used to optimize MFs in these systems. In the next section, the performances of different optimal MFs are compared in both the frequency and time domains. Then, the authors shed light on the frequency shift of superstructure, the influence of response amplifications in the NAZ and the effects of MFs in a coupled system. Eventually, the last section draws the main conclusions and presents future developments.

Modeling and transfer functions of analyzed systems

Because we are interested in generalized internal actions, i.e. base shear, bending moment, etc., the model of the superstructure, a liquid-filled tank, can be set by means of two decoupled SDOF systems as shown in Fig. 2, which represent the impulsive and convective modes of vibration of fluid (Malhotra et al., 2000). Both the mechanical and dynamic properties of the slender tank are gathered in Table 1. In order to mitigate the response of the impulsive mode of the tank, we begin with the MF proposed by Basone et al. (Basone et al., 2018). More precisely, as shown in Fig. 1(a), the unit-chain MF consists of an outer frame and massive inner resonators at floor levels, with m_j, k_j and c_j $(j = 1{,}2)$ denoting mass, stiffness and damping of the frame and the inner resonators, respectively; the configuration with 2 cells, denoted as L2H4 in (Basone et al., 2018) is adopted. Based on seismic standards, the columns of the outer frame are designed to be very flexible for isolation purposes, but to remain elastic for peak ground accelerations (PGAs) corresponding to safe shutdown earthquakes that occur once in average in 2475 years for European sites (NFPA 59A, 2016) -2% probability of exceedance in 50 years-. Hereinafter, both the damping and frequency ratio of inner resonators are reoptimized for the different systems under study, while the outer frame and the mass of resonators remain unchanged. Rayleigh damping is adopted for the frame, with 2% of equivalent critical damping for the first two modes.

As stated in the Introduction, we consider two basic systems, named System #1 and System #3 in Fig. 1(a) and Fig. 1(c), respectively. Nonetheless, to take into account the shift of frequency of the original superstructure entailed by the flexibility of the outer frame of the MF, a new system called System #2 and depicted in Fig. 1(b) is considered. It is formed by replacing the original superstructure in System #1 with an equivalent SDOF structure, which reflects the first mode of the coupled superstructure-outer frame system. The MFs optimized in these three systems are denoted as MF #1, #2 and #3, respectively.

Uncoupled systems

With regard to System #1 shown in Fig. 1(a), it is composed of two substructures: MF #1 and the superstructure. The system of equations of motion of MF #1 subjected to a base excitation $\ddot{x}_g$ can be expressed as

$$\mathbf{M}^{\mathbf{MF}}\ddot{\mathbf{x}}^{\mathbf{MF}} + \mathbf{C}^{\mathbf{MF}}\dot{\mathbf{x}}^{\mathbf{MF}} + \mathbf{K}^{\mathbf{MF}}\mathbf{x}^{\mathbf{MF}} = -\mathbf{M}^{\mathbf{MF}}\mathbf{r}^{\mathbf{MF}}\ddot{x}_g \quad (1)$$

where,

$\mathbf{M}^{\mathbf{MF}} = \begin{bmatrix} \mathbf{M}^{\mathrm{f}} & \mathbf{0} \\ \mathbf{0} & \mathbf{M}^{\mathrm{r}} \end{bmatrix}_{4\times4}$

$\mathbf{K}^{\mathbf{MF}} = \begin{bmatrix} \mathbf{K}^{\mathrm{f}} + \mathbf{K}^{\mathrm{r}} & -\mathbf{K}^{\mathrm{r}} \\ -\mathbf{K}^{\mathrm{r}} & \mathbf{K}^{\mathrm{r}} \end{bmatrix}_{4\times4}$

$\mathbf{C}^{\mathbf{MF}} = \begin{bmatrix} \mathbf{C}^{\mathrm{f}} + \mathbf{C}^{\mathrm{r}} & -\mathbf{C}^{\mathrm{r}} \\ -\mathbf{C}^{\mathrm{r}} & \mathbf{C}^{\mathrm{r}} \end{bmatrix}_{4\times4}$

$\mathbf{M}^{\mathrm{f}} = \mathrm{diag}(m_1, m_1)_{2\times2}$; $\mathbf{M}^{\mathrm{r}} = \mathrm{diag}(m_2, m_2)_{2\times2}$;

$\mathbf{K}^{\mathrm{f}} = \begin{bmatrix} 2k_1 & -k_1 \\ -k_1 & k_1 \end{bmatrix}$; $\mathbf{K}^{\mathrm{r}} = \mathrm{diag}(k_2, k_2)_{2\times2}$

$\mathbf{C}^{\mathrm{f}} = \alpha\mathbf{M}^{\mathrm{f}} + \beta\mathbf{K}^{\mathrm{f}}$; $\mathbf{C}^{\mathrm{r}} = \mathrm{diag}(c_2, c_2)_{2\times2}$

$\mathbf{x}^{\mathbf{MF}} = \left[x_1^{\mathrm{f}}\ x_2^{\mathrm{f}}\ x_1^{\mathrm{r}}\ x_2^{\mathrm{r}}\right]^{\mathrm{T}}$

$\mathbf{r}^{\mathbf{MF}} = [1\ 1\ 1\ 1]^{\mathrm{T}}$

The superscripts f and r stand for the frame and inner resonators, respectively; $\mathbf{x}^{\mathbf{MF}}$ denotes the displacement vector relative to the ground displacement $x_g(t)$. Given a harmonic acceleration excitation $\ddot{x}_g = \mathrm{e}^{\mathrm{i}\omega\mathrm{t}}$ where $\mathrm{i} = \sqrt{-1}$, the transfer function that relates the relative displacement of the system to the excitation can be expressed as

$$\mathbf{H}_{\mathrm{x}}^{\mathbf{MF}}(\omega) = \frac{\mathbf{M}^{\mathbf{MF}}\mathbf{r}^{\mathbf{MF}}}{-\omega^2\mathbf{M}^{\mathbf{MF}} + \mathrm{i}\omega\mathbf{C}^{\mathbf{MF}} + \mathbf{K}^{\mathbf{MF}}} \quad (2)$$

In addition, the transfer function of the absolute acceleration can be expressed as

$$\mathbf{H}_{a}^{\mathbf{MF}}(\omega) = 1 - \omega^2\mathbf{H}_{\mathrm{x}}^{\mathbf{MF}}(\omega) \quad (3)$$

The element of $\mathbf{H}_{a}^{\mathbf{MF}}(\omega)$ that defines the transfer function at Point 1 (the top of MF #1) is denoted as $\mathrm{H}_{\mathrm{MF1}}(\omega)$.

Given the transfer function $\mathrm{H}_{\mathrm{S}}(\omega)$ of an SDOF system,

$$H_s(\omega) = \frac{m^s}{-\omega^2 m^s + i\omega c^s + k^s} \quad (4)$$

in which m^s, k^s and c^s are the mass, stiffness and damping coefficient of the superstructure, respectively. The power spectral density (PSD) of the superstructure response $\mathrm{S}_{s1}(\omega)$ can be determined as

$$\mathrm{S}_{s1}(\omega) = |\mathrm{H}_s(\omega)|^2|\mathrm{H}_{\mathrm{MF1}}(\omega)|^2\mathrm{S}_{\ddot{x}_g}(\omega) = |\mathrm{H}_s(\omega)|^2\mathrm{S}_{\mathrm{P1}}(\omega) \quad (5)$$

where $\mathrm{S}_{\mathrm{P1}}(\omega)$ denotes the PSD of the response at Point 1 in Fig. 1(a), whilst $\mathrm{S}_{\ddot{x}_g}(\omega)$

defines the PSD of a seismic record.

As far as System #2 is concerned, see Fig. 1(b), we recall that the main characteristics of the coupled system of the original superstructure and the outer frame of the MF are dynamically represented by an equivalent SDOF system. The mass, eigenfrequency and damping ratio of the equivalent SDOF system are the corresponding parameters of the first mode of the coupled superstructure-outer frame system. As a result, the response PSD of the equivalent SDOF structure $S_{s2}(\omega)$ can be evaluated as

$$\mathrm{S}_{s2}(\omega) = \left|\mathrm{H}_{\mathrm{eq}}(\omega)\right|^2 |\mathrm{H}_{\mathrm{MF1}}(\omega)|^2 \mathrm{S}_{\ddot{x}_g}(\omega) \qquad (6)$$

where $H_{eq}(\omega)$ defines the transfer function of the equivalent SDOF structure. $H_{eq}(\omega)$ can be easily obtained by substituting the parameters of the equivalent SDOF structure into Eq. (4).

Coupled system

The coupled System #3 depicted in Fig. 1(c) is characterized by MF #3 connected to the superstructure. The relevant system of equations of motion reads,

$$\mathbf{M}\ddot{\mathbf{x}} + \mathbf{C}\dot{\mathbf{x}} + \mathbf{K}\mathbf{x} = -\mathbf{M}\mathbf{r}\ddot{x}_g \qquad (7)$$

where

$$\mathbf{M} = \begin{bmatrix} \mathbf{M}^{\mathrm{f}} & & \\ & \mathbf{M}^{\mathrm{r}} & \\ & & \mathbf{M}^{\mathrm{s}} \end{bmatrix}_{5\times 5}$$

$$\mathbf{K} = \begin{bmatrix} \mathbf{K}^{\mathrm{f}} + \mathbf{K}^{\mathrm{r}} + \mathbf{K}_1^{\mathrm{s}} & -\mathbf{K}^{\mathrm{r}} & -(\mathbf{K}_2^{\mathrm{s}})^{\mathrm{T}} \\ -\mathbf{K}^{\mathrm{r}} & \mathbf{K}^{\mathrm{r}} & \mathbf{0} \\ -\mathbf{K}_2^{\mathrm{s}} & \mathbf{0} & \mathbf{K}_3^{\mathrm{s}} \end{bmatrix}_{5\times 5}$$

$$\mathbf{C} = \begin{bmatrix} \mathbf{C}^{\mathrm{f}} + \mathbf{C}^{\mathrm{r}} + \mathbf{C}_1^{\mathrm{s}} & -\mathbf{C}^{\mathrm{r}} & -(\mathbf{C}_2^{\mathrm{s}})^{\mathrm{T}} \\ -\mathbf{C}^{\mathrm{r}} & \mathbf{C}^{\mathrm{r}} & \mathbf{0} \\ -\mathbf{C}_2^{\mathrm{s}} & \mathbf{0} & \mathbf{C}_3^{\mathrm{s}} \end{bmatrix}_{5\times 5}$$

$\mathbf{M}^{\mathrm{s}} = m^{\mathrm{s}}$;

$\mathbf{K}_1^{\mathrm{s}} = \mathrm{diag}(0,0,k^{\mathrm{s}})_{3\times 3}$; $\mathbf{K}_2^{\mathrm{s}} = [0,0,k^{\mathrm{s}}]_{1\times 3}$; $\mathbf{K}_3^{\mathrm{s}} = k^{\mathrm{s}}$;

$\mathbf{C}_1^{\mathrm{s}} = \mathrm{diag}(0,0,c^{\mathrm{s}})_{3\times 3}$; $\mathbf{C}_2^{\mathrm{s}} = [0,0,c^{\mathrm{s}}]_{1\times 3}$; $\mathbf{C}_3^{\mathrm{s}} = c^{\mathrm{s}}$;

$\mathbf{x} = \left[x_1^{\mathrm{f}}\ x_2^{\mathrm{f}}\ x_1^{\mathrm{r}}\ x_2^{\mathrm{r}}\ x^{s}\right]^{\mathrm{T}}$; $\mathbf{r} = [1\ 1\ 1\ 1\ 1]^{\mathrm{T}}$

The transfer function of the absolute acceleration of System #3 can be derived as

$$\mathbf{H}_{\boldsymbol{a}}(\omega) = 1 - \omega^2 \mathbf{H}_{\mathrm{x}}(\omega) \tag{8}$$

in which

$$\mathbf{H}_{\mathrm{x}}(\omega) = \frac{\mathbf{Mr}}{-\omega^2 \mathbf{M} + \mathrm{i}\omega \mathbf{C} + \mathbf{K}} \tag{9}$$

The transfer function of the absolute acceleration of the superstructure at Point 4 w.r.t. the excitation is the last element of $\mathbf{H}_{\mathrm{x}}(\omega)$, denoted as $\mathrm{H}_4(\omega)$**.** As a result, the PSD of the superstructure's response of System #3 $\mathrm{S}_{s3}(\omega)$ can be determined as,

$$\mathrm{S}_{s3}(\omega) = |\mathrm{H}_4(\omega)|^2 \mathrm{S}_{\ddot{x}_g}(\omega) \tag{10}$$

Optimization of metafoundations

In order to deal with meaningful results, in what follows we optimize the inner resonators of each MF presented in the three systems depicted in Fig. 1 . Therefore, we assume that the ground displacement $x_g(t)$ is a weakly stationary process such that the autocorrelation functions of the system response, defined in terms of statistical expected values, can be computed with the Wiener–Khinchin theorem (Soong and Grigoriu, 1993).

Ground motion selection

In order to select proper sets of accelerograms and relevant weakly stationary power spectra, a specific active prone-site, Priolo Gargallo, Italy, was selected (Basone et al., 2018). For simplicity, one set of natural accelerograms that occur once in average in 475 years -10% probability of exceedance in 50 years- was chosen, see Table 2, corresponding to operating basis earthquakes (OBE). For clarity, the OBE can be defined as the ground motion for which those features of process plant components necessary for continued operation without risk to the health and safety of the public will remain fully functional. Conversely, safe shutdown earthquakes are the ground motions in which certain structures, systems and components important for safe shutdown must be designed to remain operational. Moreover, the 15 natural accelerograms were selected to best fit in average the uniform hazard response spectrum (UHS) of the site, as shown in Fig. 3. It is well known that the UHS is often overly conservative because it combines the hazard from different sources and does not reflect a realistic spectrum that can be expected to occur during a single earthquake. However, the use of a conditional mean spectrum that matches the UHS level only at the fundamental period of a system is overly complex for the problem to hand. Then, in order to define the PSD functions in Eqs. (5), (6) and (10), which characterize the weakly stationary OBE events, we evaluated the parameters of the Kanai-Tajimi filter modified by Clough and Penzien, denoted as KC filter. Its magnitude reads

$$|\mathrm{H}_{\mathrm{KC}}(\omega)|^2 = |\mathrm{H}_{\mathrm{KT}}(i\omega)|^2 |\mathrm{H}_{\mathrm{CP}}(i\omega)|^2 \qquad (11)$$

where

$$\mathrm{H}_{\mathrm{KT}}(\omega) = \frac{\omega_g^2 + 2i\xi_g\omega_g\omega}{(\omega_g^2 - \omega^2) + 2i\xi_g\omega_g\omega} \qquad (12)$$

$$\mathrm{H}_{\mathrm{CP}}(\omega) = \frac{\omega^2}{(\omega_f^2 - \omega^2) + 2i\xi_f\omega_f\omega} \qquad (13)$$

The parameters ω_g and ξ_g in Eq. (12) represent the frequency and damping properties, respectively, of the supporting ground modeled by an SDOF system. Conversely, the parameters ω_f and ξ_f Eq. (13) control the cut-off frequency and the steepness of a high-pass filter used to suppress the low-frequency content (Giaralis and Taflanidis, 2017). Relevant parameters of the KC-fitted PSD for the OBE are $[\omega_g, \xi_g, \omega_f, \xi_f, S_0] = [12.0\, rad/s, 0.60, 2.0\, rad/s, 0.62, 0.037\, m^2/s^3]$, where S_0 defines the spectral intensity of the stationary white noise process.

Optimization procedure

The autocovariance or variance of the superstructure absolute acceleration $\sigma_a^{2,CON}$ of each controlled system can be calculated by the Wiener–Khinchin theorem, as

$$\sigma_a^{2,CON} = E[a^2(\tau = 0)] = \int_0^\infty \mathrm{S}_{si}(\omega)\, d\omega \quad (i = 1, 2, 3) \qquad (14)$$

where $E[a^2(\tau = 0)]$ defines the expectation of the random variable a and τ is the time lag (Vanmarcke, 1976; Kjell, 2002). The variance of the uncontrolled superstructure can be obtained as

$$\sigma_a^{2,UNC} = \int_0^\infty |\mathrm{H}_s(\omega)|^2 \mathrm{S}_{\ddot{x}_g}(\omega)\, d\omega \quad (15)$$

Then, a variance ratio can be defined as

$$\gamma_{\sigma^2} = \sigma_a^{2,CON} / \sigma_a^{2,UNC} \quad (16)$$

The variance ratio γ_{σ^2}, which is commonly used as the objective function in the optimization of passive structural vibration control, see among others (De Domenico and Ricciardi, 2018), is selected as the objective function. By replacing $S_{\ddot{x}_g}(\omega)$ in Eq. (5), (6), (10) and (15) with the KC-fitted PSD for the OBE accelerograms obtained in Section “Ground motion selection”, an optimization in the frequency domain was carried out. As a result, in order to achieve the maximum attenuation of the variance ratio γ_{σ^2} based on the construction site, γ_{σ^2} was minimized in the frequency domain. Since the outer frame of each MF must be as flexible as possible to act as base isolation whilst the mass m_2 of each inner resonator has to be as large as possible to lower the frequency limits of the AZ (Dertimanis et al., 2016), both the damping ratio $\xi_2 = \frac{c_2}{2m_2\omega_2}$ and the frequency ratio $\gamma_\omega = \omega_2/\omega_s$ (where $\omega_2 = \sqrt{k_2/m_2}$) of resonators can be assumed as design variables. As a result, the optimization problem can be posed as follows:

Find the design vector $\mathbf{d} = [\xi_2, \gamma_\omega]$, to get min γ_{σ^2}, subject to the bounds $0.01 \leq \xi_2 \leq 0.3$ and $0.1 \leq \gamma_\omega \leq 1.5$

The optimization problem can be solved by using the genetic algorithm function in MATLAB. Relevant optimal design variables are collected in Table 3.

Performance of optimized systems

In this section, the performance of the aforementioned optimized systems is evaluated in both the time and frequency domains.

Let’s define the ratio of peak responses of both the controlled and uncontrolled superstructure γ_{Resp}, which is conceived to evaluate mitigation performance of MFs in the time domain. In particular, γ_{Resp} is defined as

$$\gamma_{\mathrm{Resp}} = \frac{\max(a_j^{CON})}{\max(a_j^{UNC})} \tag{17}$$

where $\max(a_j^{CON})$ and $\max(a_j^{UNC})$ are the maximum absolute accelerations of the controlled and uncontrolled superstructures, respectively, subjected to the j^{th} OBE. More precisely, γ_{Resp} is evaluated in the uncoupled System #1 endowed with MF #1; relevant values are compared in Table 4 with those of the coupled system.

When MF #1 is used in an uncoupled system, a certain mitigation effect is achieved, as indicated by the first column of Table 4. However, if it is used in a coupled system its performance declines, due to the frequency shift of the superstructure, as indicated by the second column of Table 4. A more in-depth explanation of this phenomenon is provided in the next section.

With regard to the performance of the three MFs in the coupled system, the best mitigation effect is provided by MF #3, because MF #3 is directly optimized for the whole system. More precisely, as indicated in Table 4, a 23% average mitigation effect is achieved by MF #3 while that for MF #2 is 18% and MF #1 is ineffective in the average. The standard deviation of MF #3 is the lowest of the three MFs. The number of accelerograms that amplify the controlled superstructure response in the case of MF #3 is also minimal. All these figures indicate a more effective and stable mitigation effect of MF #3. Conversely, the mitigation effect of MF #1 is the worst. As far as the performance of MF #2 is concerned, this metafoundation, which is optimized in the uncoupled system but based on an equivalent SDOF, can achieve a performance close to that of MF #3.

With reference to the frequency domain, the moduli of transfer functions of superstructures $|\mathrm{H}_{4,\mathrm{j}}(\omega)|$ in coupled systems with the three optimal MFs are presented in Fig. 4. Anew, MF #3 is the most effective in terms of amplitude reduction, as indicated by the transfer function amplitude of the superstructure with MF #3 $|\mathrm{H}_{4,3}(\omega)|$; this is consistent with the results of Table 4. Conversely, only a limited benefit is achieved with MF #1. It is noteworthy to mention that $|\mathrm{H}_{4,2}(\omega)|$ and

$|H_{4,3}(\omega)|$ exhibit two peaks due to the AZ caused by the inner resonators while $|H_{4,1}(\omega)|$ shows only a single peak entailed by the superstructure.

System analysis

In this section, we investigate the dynamic effects of MFs. Based on the uncoupled system, the coupling effect of NAZ and AZ on seismic mitigation effects is clearly illustrated. Moreover, the effect of the frequency shift of superstructure is investigated by comparing System #1 - #2 of Fig. 1. Then the mechanism of MFs in a coupled structure is discussed.

Amplification in non-atteunation zones

Fig. 5 displays the PSD $S_{P1}(\omega)$ at Point 1, see Fig. 1(a), and that of the corresponding input at the base of MF #1, $S_{\ddot{x}_g}(\omega)$. The AZ of MF #1 is marked with a shade area and other frequency components of the metafoundation response in NAZ are clearly amplified. Based on the well-known modal superposition method (Chandra Rao et al., 2002), $H_{MF1}(\omega)$ of MF #1 can be expressed as,

$$H_{MF1}(\omega) = \left| \sum_{j=1}^{4} \phi_{j,2}\gamma_j(1+\omega^2)H_j(\omega) \right| \quad (18)$$

where

$$H_j(\omega) = \frac{1}{\omega_j^2 - \omega^2 + 2i\xi_j\omega_j\omega} \quad (19)$$

defines the modal transfer function that relates the relative displacement of the equivalent SDOF system of the j^{th} mode of MF #1 to excitations; ω_j and ξ_j, denote the natural frequency and damping ratio in the j^{th} primary mode, respectively; $\{\phi_j\}$ is the j^{th} mode shape and $\phi_{j,2}$ is the element corresponding to the top of MF #1.

Eq. (18) singles out the contribution of each mode that characterizes the response of MF #1. Moreover, Fig. 6 displays $|H_{MF1}(\omega)|$ and the contributions of its 1st and 3rd

mode, respectively. It is evident that amplifications in NAZs are mainly caused by the inner resonators -1st mode - and outer frame -3rd mode-. The second mode reflects the antiresonance or AZ.

Quantification of non-attenuation zones and attenuation zones

In order to quantify the response contribution relevant to both NAZ and AZ, we can use σ_a^2 evaluated by Eq. (14). Furthermore, a standard deviation ratio γ_σ is defined as $\gamma_\sigma = \sigma_a^{CON}/\sigma_a^{UNC}$, where σ_a^{CON} and σ_a^{UNC} are the standard deviations of responses of the controlled superstructure in System #1, see Fig. 1(a), and the uncontrolled superstructure, respectively. A correlation exists between the standard deviation σ_a of an SDOF system response subjected to a seismic record and its maximum response. The plot that correlates γ_σ and γ_{Resp} is presented in Fig. 7 for System #1, subjected to the seismic records listed in Table 2. We can define a linear regression equation, i.e., $\gamma_{\mathrm{Resp}} = 1.046\gamma_\sigma + 0.045$ with a coefficient of determination $R^2 = 0.8$. The correlation is relatively good. Hence, the maximum response ratio γ_{Resp} can be evalutated from the standard deviation ratio γ_σ.

As γ_σ is related to both PSD function of the response and approximately to γ_{Resp}, in order to quantify response contributions of the NAZ and AZ, the area ratios of PSD of these zones are selected as indexes, i.e.,

$$\gamma_A^{NAZ} = \frac{\int_{NAZ} S_{s1}(\omega)\, d\omega}{\int_0^\infty S_{s1}(\omega)\, d\omega}, \gamma_A^{AZ} = \frac{\int_{AZ} S_{s1}(\omega)\, d\omega}{\int_0^\infty S_{s1}(\omega)\, d\omega} \qquad (20)$$

The corresponding results are depicted in Fig. 8, where the yellow bar defines the response ratio of the controlled and uncontrolled superstructures γ_{Resp}. The blue bar indicates the PSD relevant to the NAZ divided by the total area of the response PSD, γ_A^{NAZ}. In the same way, the green bar indicates the same quantity for the AZ, γ_A^{AZ}. From Fig. 8, a careful reader can observe that the NAZ for System #1 prevails in five records, that is, N. 2, 3, 7, 8 and 15; therefore, the response of the controlled superstructure is amplified in these cases. Conversely, the AZ and the relevant mitigation effects prevail in records 11, 12 and 14. In sum, the contribution of NAZ is quite important when MF #1 is employed to mitigate seismic response of a superstructure.

Frequency shift of superstructure

The mitigation performance of MFs can benefit from the use of a flexible unit cell – flexible outer frame- which entails an isolation effect due to a superstructure frequency shift. However, this shift hindered the mitigation performance of MF #1 in the coupled system. More precisely, MF #1 has been optimized in the uncoupled system. Therefore, it realizes an AZ which covers the eigenfrequency of the uncontrolled superstructure (dashed line), marked with a shaded area in Fig. 9. Nonetheless, when MF #1 is involved in the coupled system, due to coupling, the eigenfrequency of the superstructure shifts to a lower frequency value which results to be outside the AZ of MF #1. See, in this respect, the continuous line of the coupled system with MF #1. As a result, MF #1 fails to mitigate the seismic response of the superstructure in the coupled system.

MF #2 depicted in Fig. 1(b) is also optimized in the uncoupled system. However, in order to take into account the aforementioned frequency shift, instead of the original superstructure an equivalent SDOF system is used. Therefore, MF #2 exhibits an AZ that covers the eigenfrequency component of the equivalent SDOF, as shown in Fig. 10. As a result, the peak frequency of the superstructure in the coupled system with MF #2, see the second peak of the continuous line of the coupled system with MF #2 in Fig. 10, actually falls into the AZ. Therefore, a more favorable mitigation effect is achieved with MF #2, w.r.t. the previous coupled system with MF #1.

Performance of metafoundations in System #3

MF #3 is directly optimized through the whole coupled system #3, as shown in Fig. 1(c), and thus it achieves the most effective mitigation effect compared with the previous MFs. More precisely, Fig. 11 displays the transfer function modulus of the superstructure at Point 4 controlled with MF #3 (continuous line) and that of MF #3 at Point 3 (dashed line). Similarly to the mechanism explained for MF #2 through Fig. 12, the eigenfrequency component of the controlled superstructure, reflected by the second peak of the coupled system with MF #3 at Point 4, falls into the AZ of MF #3 alone. Moreover, one can observe that the response of the coupled system endowed with MF #3 at Point 3, see Fig. 1(c), determines the mitigation effect on the superstructure.

Furthermore, the eigenfrequencies of all modes and the corresponding normalized modal participation masses of coupled systems with MF #2 and #3, respectively, are listed in Table 5. A careful reader can observe that the dynamic characteristics of these two systems are similar. However, a more favorable mitigation effect is obtained with MF #3 because $\left|H_{4,3}(\omega)\right|$ with MF #3, see Fig. 4, has more favorable characteristics in terms of peak amplitude equality than $\left|H_{4,2}(\omega)\right|$ with MF #2. The first peaks of the two aforementioned transfer functions moduli reflect amplifications in the NAZs, as explained for the uncoupled system. Eventually, System #3 with the optimized MF #3 achieves a better mitigation effect due to a proper combination between NAZ and AZ.

Conclusions

In this paper, in order to understand the seismic mitigation of coupled systems made of periodic foundations and superstructures, analysis tools in both the frequency and time domain were applied on the new concept of finite locally resonant optimal metafoundations (MFs). This was achieved by modeling MFs as a finite one-dimensional unit-cell chain endowed with massive inner resonators. The resulting mitigation effect derives from attenuation effects entailed by unit cells and eigenfrequency shifts induced by flexible unit cells. In order to explain these effects, two types of systems, uncoupled and coupled systems are employed. As a result, response amplification in both non-attenuation (NAZs) and attenuation zones (AZ) and eigenfrequency shifts of superstructures are discussed in depth. Moreover, to address uncertainty at the excitation level, time history analyses were carried out with a set of natural accelerograms that characterize operating basis earthquakes; thus, both response contributions of AZs and NAZs can be distinguished by relating response variances and peak responses.

More precisely, we considered three specific MFs that are optimized in an uncoupled system -MF #1-, in an uncoupled system using an equivalent SDOF superstructure -MF #2- and in the coupled system -MF #3-. Based on the results achieved with MF #1, we have illustrated that seismic mitigation effects depend on both attenuations in AZs and amplification in NAZs. The amplification of some frequency components in NAZs results from resonances of some eigenmodes of the MF. Moreover, with the help of MF #2, the effect of the frequency shift of the superstructure due to the flexible outer frame of MF #2 was illustrated. Furthermore, the performance of MF #3 was discussed. It was directly optimized in a coupled system and achieved the most effective mitigation effect. This results from a combination of base-isolation effects, a wider AZ due to coupling and the best balance between AZ and NAZs. It is noteworthy to mention that the analysis becomes more challenging for a more complex MF with added independent resonators, because local optimal solutions increase. These MFs will be the subject of a future study.

Data Availability Statement

Some or all data, models, or code generated or used during the study are available from the corresponding author by request:

The code used to calculate transfer functions and time-history responses

Acknowledgements

The first two authors greatly acknowledge the financial support by National Natural Science Foundation of China (No. 51778488).

The last author acknowledges the funding received from the European Union’s Horizon 2020 SERA: Seismology and Earthquake Engineering Research Infrastructure Alliance for Europe (Grant No: 730900); and the Italian Ministry of 460 Education, University and Research (MIUR) in the frame of the ”Departments of Excellence” (grant L. 232/2016).

References

MATLAB R2017a. The MathWorks, Inc., Natick, Massachusetts, United States.

Achaoui Y, Ungureanu B, Enoch S, et al. (2015) Seismic waves damping with arrays of inertial resonators. *Extreme Mechanics Letters* 8: 30-37.

Bao J, Shi Z and Xiang H. (2012) Dynamic Responses of a Structure with Periodic Foundations. *Journal of Engineering Mechanics-Asce* 138: 761-769.

Basone F, Wenzel M, Bursi OS, et al. (2018) Finite locally resonant Metafoundations for the seismic protection of fuel storage tanks. *Earthquake Engineering & Structural Dynamics*.

Brûlé S, Javelaud EH, Enoch S, et al. (2014) Experiments on seismic metamaterials: molding surface waves. *Phys.rev.lett* 112: 133901.

Casablanca O, Ventura G, Garescì F, et al. (2018) Seismic isolation of buildings using composite foundations based on metamaterials. *Journal of Applied Physics* 123: 174903.

Chandra Rao VS, Chaudhuri SR and Gupta VK. (2002) Mode-acceleration approach to seismic response of multiply - supported secondary systems. *Earthquake Engineering & Structural Dynamics* 31: 1603-1621.

Cheng Z and Shi Z. (2018a) Composite periodic foundation and its application for seismic isolation. *Earthquake Engineering & Structural Dynamics* 47: 925-944.

Cheng ZB and Shi ZF. (2013) Novel composite periodic structures with attenuation zones. *Engineering Structures* 56: 1271-1282.

Cheng ZB and Shi ZF. (2018b) Composite periodic foundation and its application for seismic isolation. *Earthquake Engineering & Structural Dynamics* 47: 925-944.

Colombi A, Colquitt D, Roux P, et al. (2016a) Forests as a natural seismic metamaterial: Rayleigh wave bandgaps induced by local resonances. *Scientific Reports* 6: 19238.

Colombi A, Colquitt D, Roux P, et al. (2016b) A seismic metamaterial: The resonant metawedge. *Scientific Reports* 6.

De Domenico D and Ricciardi G. (2018) Optimal design and seismic performance of tuned mass damper inerter (TMDI) for structures with nonlinear base isolation systems. *Earthquake Engineering & Structural Dynamics* 47: 2539-2560.

Dertimanis VK, Antoniadis IA and Chatzi EN. (2016) Feasibility analysis on the attenuation of strong ground motions using finite periodic lattices of mass-in-mass barriers. *Journal of Engineering Mechanics*: 04016060.

Finocchio G, Casablanca O, Ricciardi G, et al. (2014) Seismic metamaterials based on isochronous mechanical oscillators. *Applied Physics Letters* 104.

Geng Q, Zhu S and Chong KP. (2018) Issues in design of one-dimensional metamaterials for seismic protection. *Soil Dynamics and Earthquake Engineering* 107: 264-278.

Giaralis A and Taflanidis AA. (2017) Optimal tuned mass-damper-inerter (TMDI) design for seismically excited MDOF structures with model uncertainties based on reliability criteria. *Structural Control & Health Monitoring* 25: e2082.

Huang J, Shi Z, Huang W, et al. (2017) A periodic foundation with rotational oscillators for extremely low-frequency seismic isolation: analysis and experimental verification. *Smart Materials and Structures* 26.

Hussein MI, Leamy MJ and Ruzzene M. (2014) Dynamics of Phononic Materials and Structures:

Historical Origins, Recent Progress, and Future Outlook. *Applied Mechanics Reviews* 66.

Kim SH and Das MP. (2012) Seismic waveguided of metamaterials *Modern Physics Letters B* 26: 8.

Kjell G. (2002) Predicting response spectra for earthquake signals generated as filtered noise. *Probabilistic Engineering Mechanics* 17: 241-252.

Krödel S, Thomé N and Daraio C. (2015) Wide band-gap seismic metastructures. *Extreme Mechanics Letters* 4: 111-117.

La Salandra V, Wenzel M, Bursi OS, et al. (2017) Conception of a 3D Metamaterial-Based Foundation for Static and Seismic Protection of Fuel Storage Tanks. *Frontiers in Materials* 4.

Liu Z, Zhang X, Mao Y, et al. (2000) Locally resonant sonic materials. *Science* 289: 1734-1736.

Malhotra PK, Wenk T and Wieland M. (2000) Simple procedure for seismic analysis of liquid-storage tanks. *Structural Engineering International* 10: 197-201.

Miniaci M, Krushynska A, Bosia F, et al. (2016) Large scale mechanical metamaterials as seismic shields. *New Journal of Physics* 18: 083041.

Palermo A, Krödel S, Marzani A, et al. (2016) Engineered metabarrier as shield from seismic surface waves. *Scientific Reports* 6: 39356.

Palermo A, Vitali M and Marzani A. (2018) Metabarriers with multi-mass locally resonating units for broad band Rayleigh waves attenuation. *Soil Dynamics and Earthquake Engineering* 113: 265-277.

Soong TT and Grigoriu M. (1993) Random vibration of mechanical and structural systems.

NASA STI/Recon Technical Report A 93.

Vanmarcke EH. (1976) Chapter 8–Structural Response to Earthquakes. *Developments in Geotechnical Engineering* 15: 287-337.

Wagner PR, Dertimanis VK, Chatzi EN, et al. (2018) Robust-to-uncertainties optimal design of seismic metamaterials. *Journal of Engineering Mechanics* 144.

Wang P, Casadei F, Shan S, et al. (2014) Harnessing buckling to design tunable locally resonant acoustic metamaterials. *Physical Review Letters* 113: 014301.

Xiang HJ, Shi ZF, Wang SJ, et al. (2012) Periodic materials-based vibration attenuation in layered foundations: experimental validation. *Smart Materials & Structures* 21: 481-484.

Yan Y, Cheng Z, Menq F, et al. (2015) Three dimensional periodic foundations for base seismic isolation. *Smart Materials and Structures* 24: 11.

Yan Y, Laskar A, Cheng Z, et al. (2014) Seismic isolation of two dimensional periodic foundations. *Journal of Applied Physics* 116: 12.

Table 1 Mechanical and dynamic properties of the slender tank

Diameter, m	8.0	Max. liquid height/Diam.	1.5
Wall thickness, mm	6	Impulsive mass, kg	5.08×10^5
Tank height, m	14.0	Impulsive frequency, Hz	6.49
Maximum liquid height, m	12.0	Height of impulsive mass, m	5.44

Table 2 List of natural accelerograms for OBE events

Number of Accelerogram	Event	ID	M	RJb [km]	PGA [m/s^2]
1	Loma Prieta	LOMAP_BRN090	6.93	3.85	0.4067
2	Kalamata	000414ya	5.9	11	0.3738
3	South Iceland	004673ya	6.5	15	0.4224
4	L'Aquila Mainshock	IT0792ya	6.3	4.87	0.6287
5	FRIULI 2ND SHOCK	IT0078ya	5.6	26.21	0.4023
6	Northridge-01	NORTHR_ORR360	6.69	20.11	0.3749
7	Umbria Marche	000594ya	6	11	0.4224
8	Montenegro	000199ya	6.9	16	0.3071
9	Erzincan	000535ya	6.6	13	0.4224
10	Friuli Italy-01	FRIULLA_A-	6.5	14.97	0.2585

		TMZ270			
11	South Iceland (after shock)	006328ya	6.4	12	0.3914
12	Ano Liosia	001715ya	6	14	0.3103
13	L'Aquila Mainshock	IT0789ya	6.3	4.63	0.4024
14	L'Aquila Mainshock	IT0790ya	6.3	4.39	0.4459
15	L'Aquila Mainshock	IT0791ya	6.3	5.65	0.33

Table 3 Optimal results for the three MFs

	MF #1	**MF #2**	**MF #3**
γ_{σ^2}	0.611	0.948	0.436
γ_{ω}	0.806	0.886	0.493
ξ_2	0.020	0.011	0.029
f_2, Hz	5.36	3.70	3.28

Table 4 Statistics of γ_{Resp} of different MFs in different systems

Statistics of γ_{Resp}	Uncoupled System with MF #1	Coupled System		
		with MF #1	with MF #2	with MF #3
Mean	0.93	1.16	0.82	0.77
Standard deviation	0.26	0.60	0.52	0.38
Minimum value	0.56	0.51	0.29	0.30
Maximum value	1.38	2.68	2.02	1.64
Number of accel. with γ_{Resp}>1	5	7	4	4

Table 5 Modal properties of coupled systems endowed with MF #2 and MF #3

Mode number	Coupled system with MF #2		Coupled system with MF #3	
	f (Hz)	Normalized γ_s	f (Hz)	Normalized γ_s
1st	3.166	0.784	2.931	0.688
2nd	3.649	0.023	3.243	0.022
3rd	4.700	0.167	4.534	0.263
4th	25.219	0.023	24.996	0.024
5th	44.265	0.003	44.137	0.003

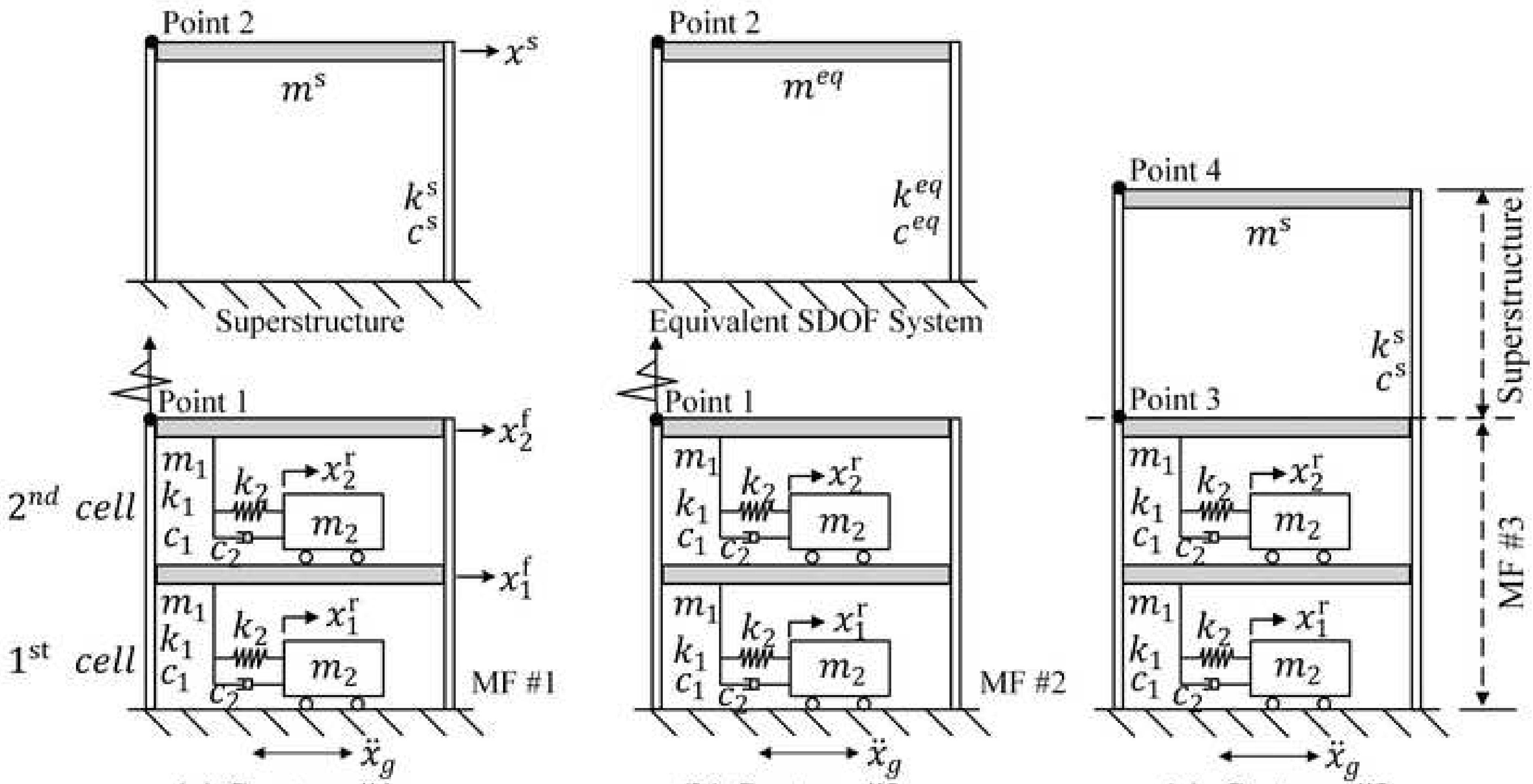

(a) System #1 (b) System #2 (c) System #3

Uncoupled system Coupled system

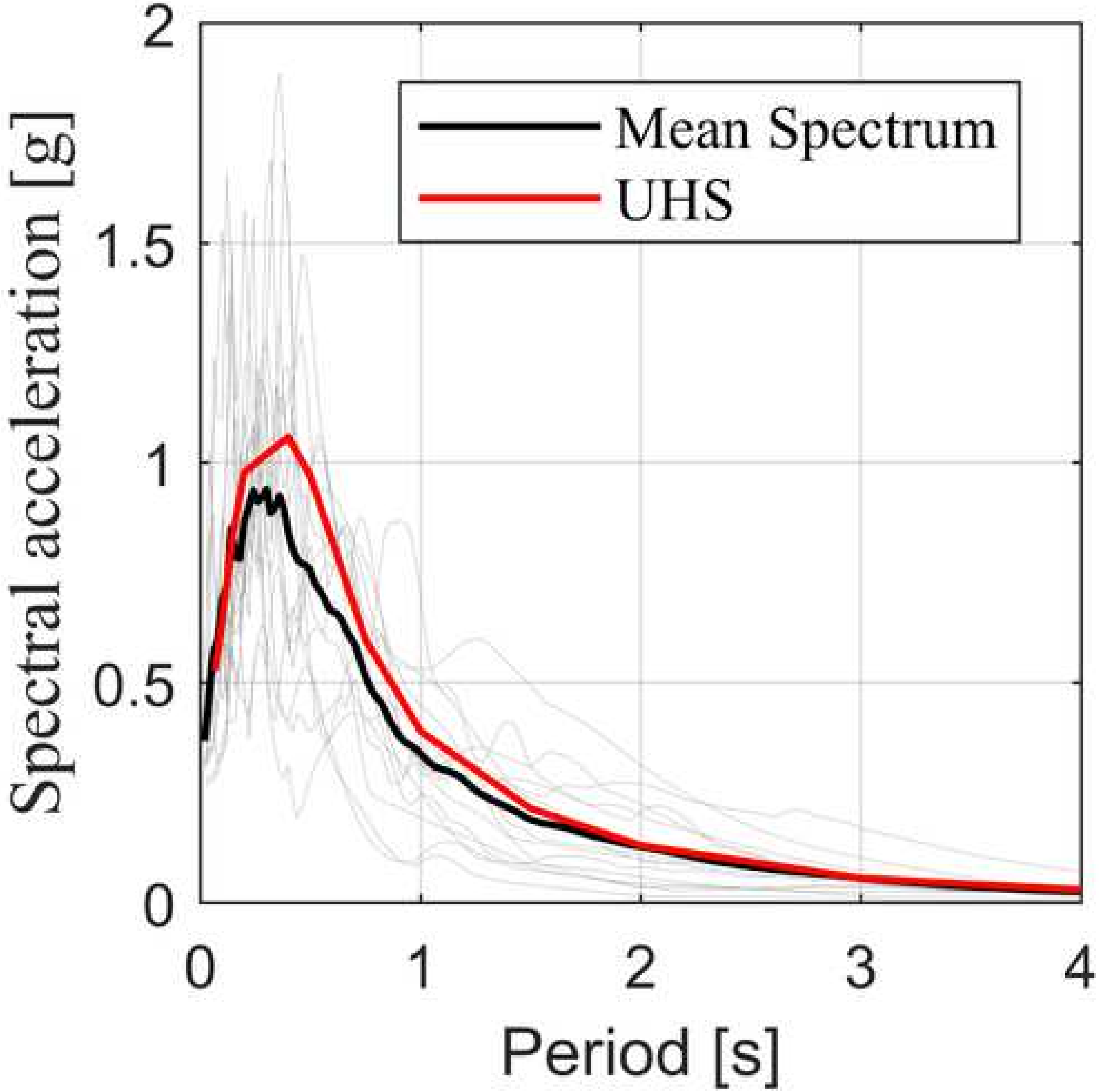

Mean Spectrum
UHS
Spectral acceleration [g]
Period [s]
0
0.5
1
1.5
2
0
1
2
3
4

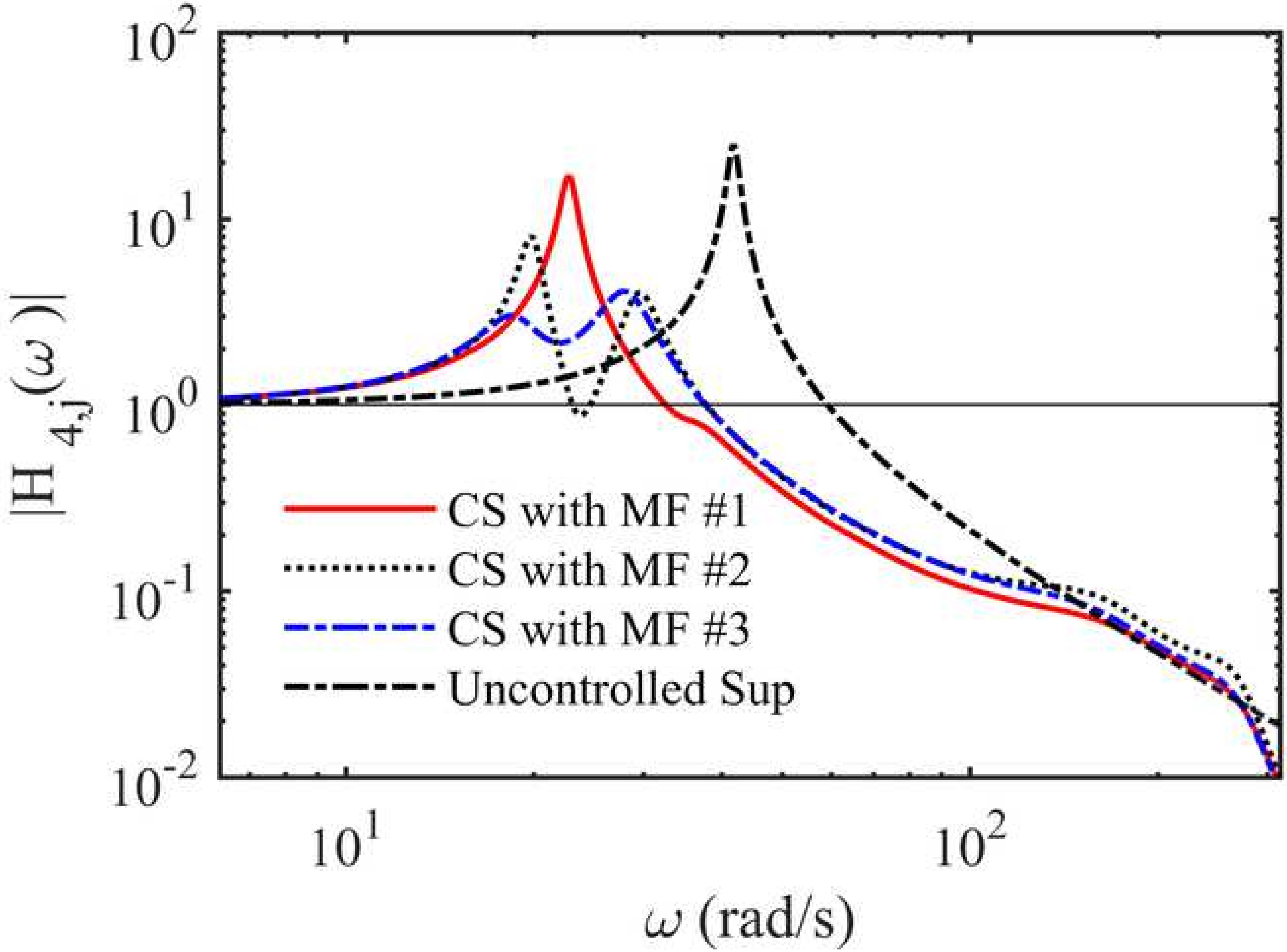
10^2
10^1
10^0
10^{-1}
10^{-2}
$|H_{4,j}(\omega)|$
CS with MF #1
CS with MF #2
CS with MF #3
Uncontrolled Sup
10^1
10^2
ω (rad/s)

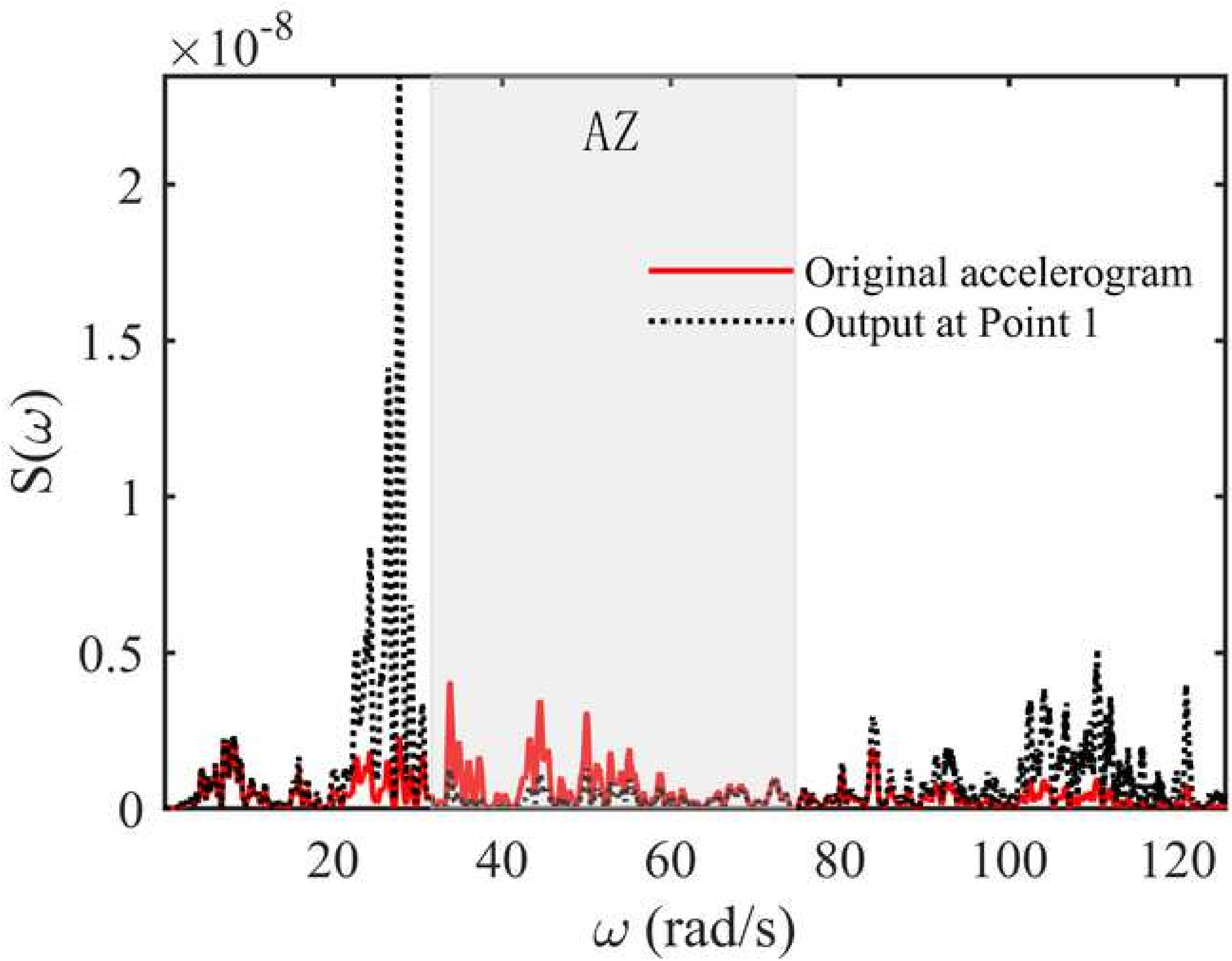
×10^-8
AZ
Original accelerogram
Output at Point 1
0
0.5
1
1.5
2
S(ω)
20
40
60
80
100
120
ω (rad/s)

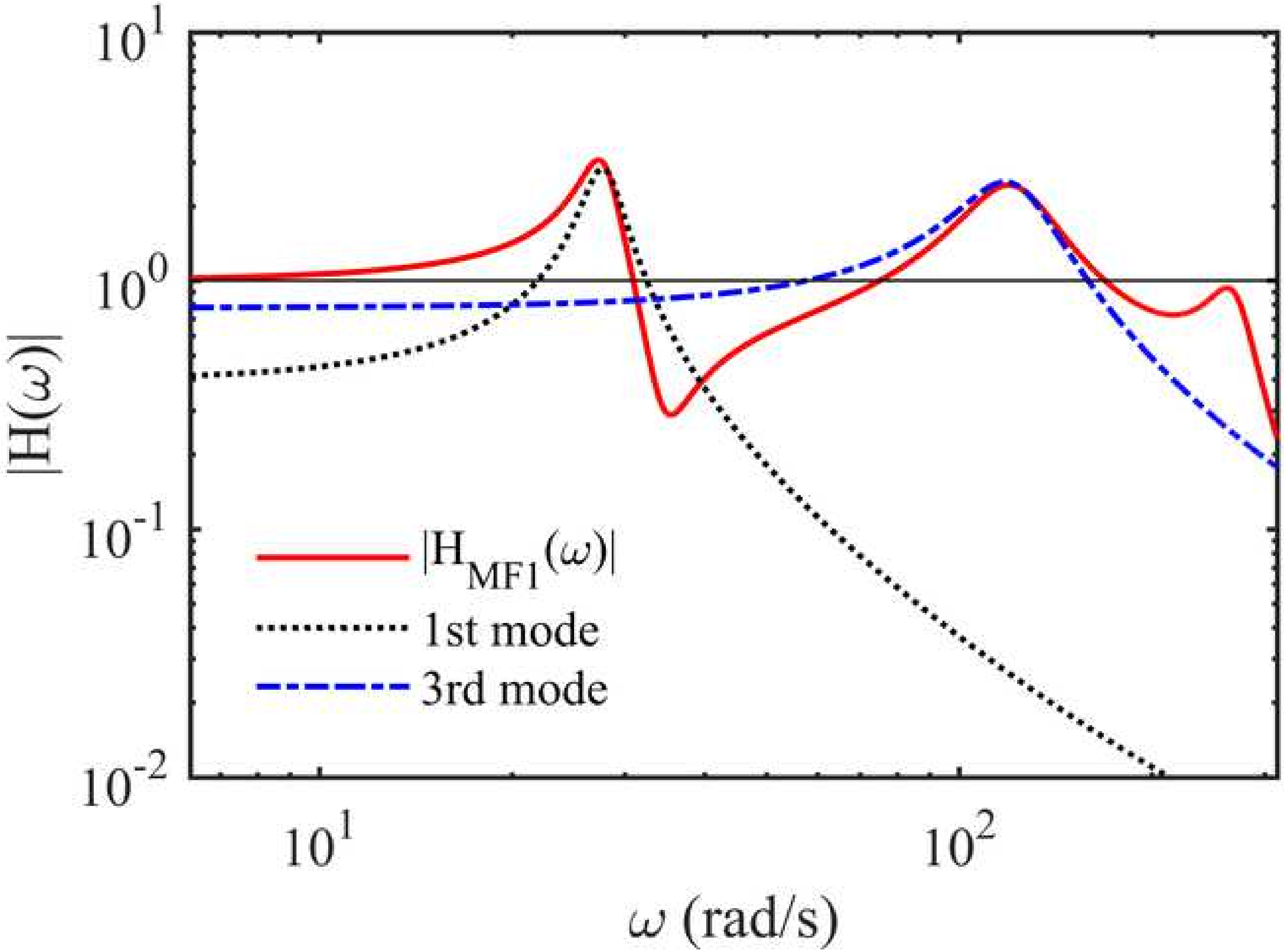

10^1
10^0
10^{-1}
10^{-2}
$|H(\omega)|$
10^1
10^2
ω (rad/s)
$|H_{MF1}(\omega)|$
1st mode
3rd mode

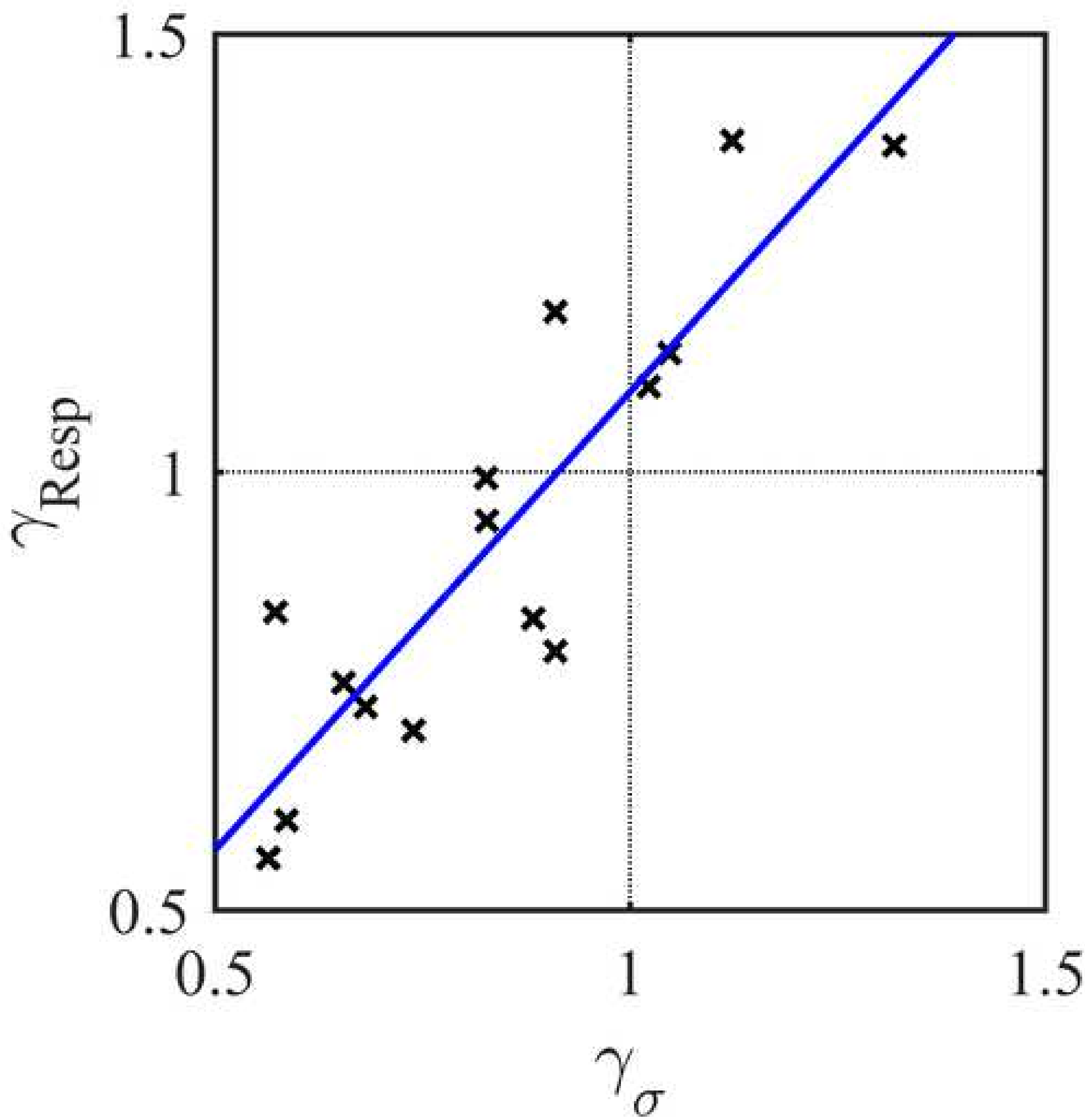
1.5
1
0.5
0.5
1
1.5
γ_{Resp}
γ_{σ}

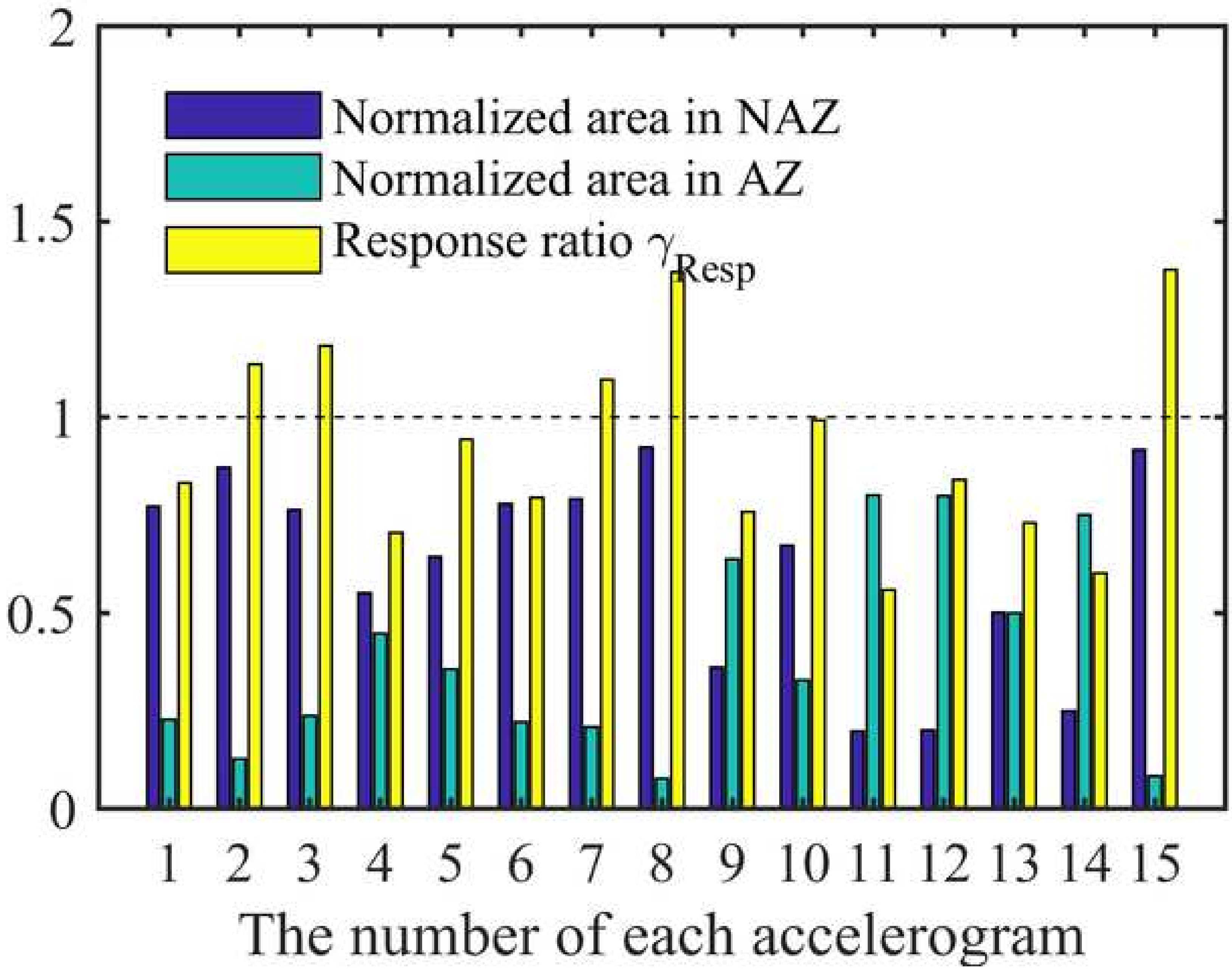

2
1.5
1
0.5
0
Normalized area in NAZ
Normalized area in AZ
Response ratio γ_{Resp}
1 2 3 4 5 6 7 8 9 10 11 12 13 14 15
The number of each accelerogram

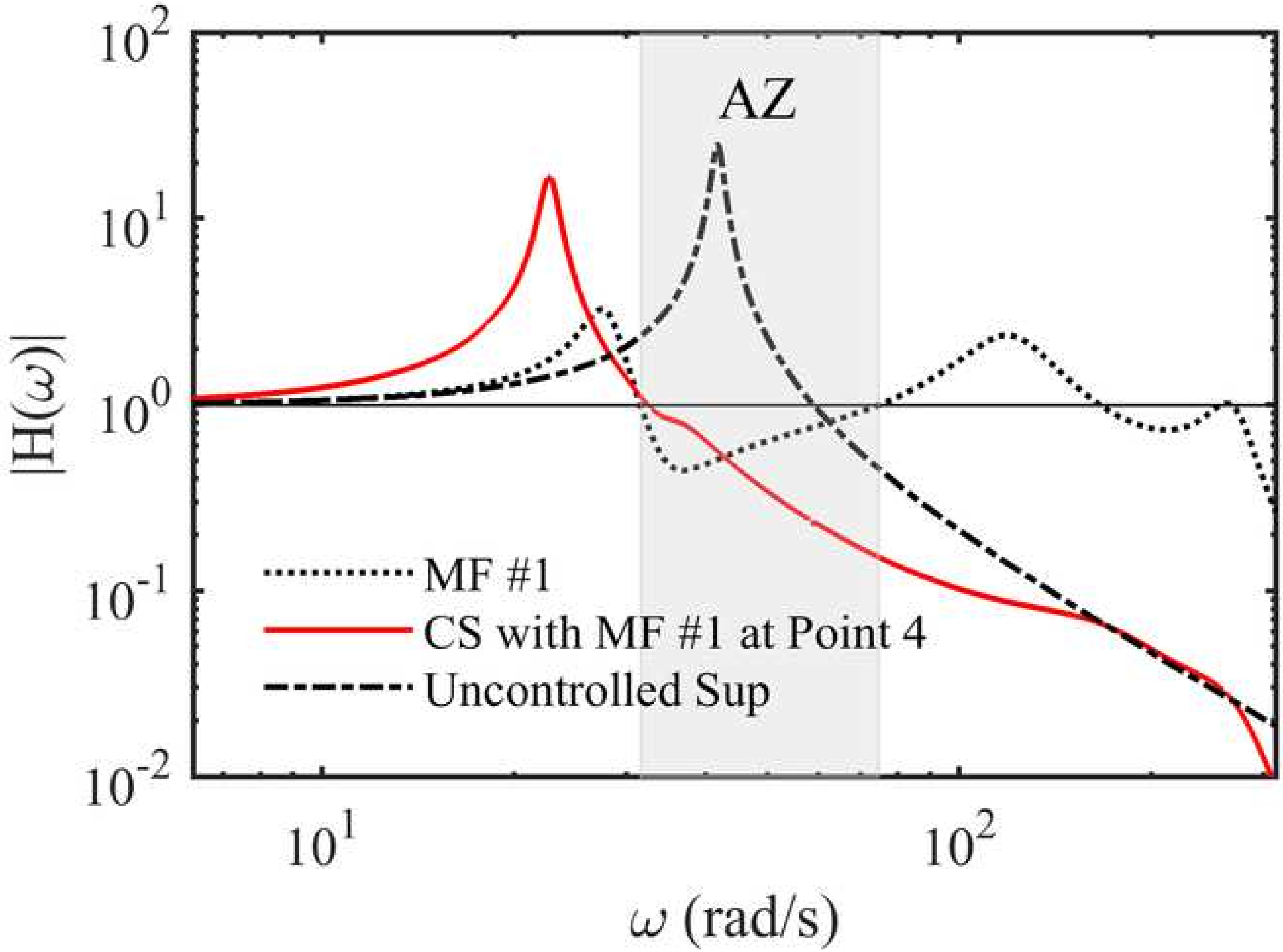
AZ
MF #1
CS with MF #1 at Point 4
Uncontrolled Sup
10^2
10^1
10^0
10^{-1}
10^{-2}
$|H(\omega)|$
10^1
10^2
ω (rad/s)

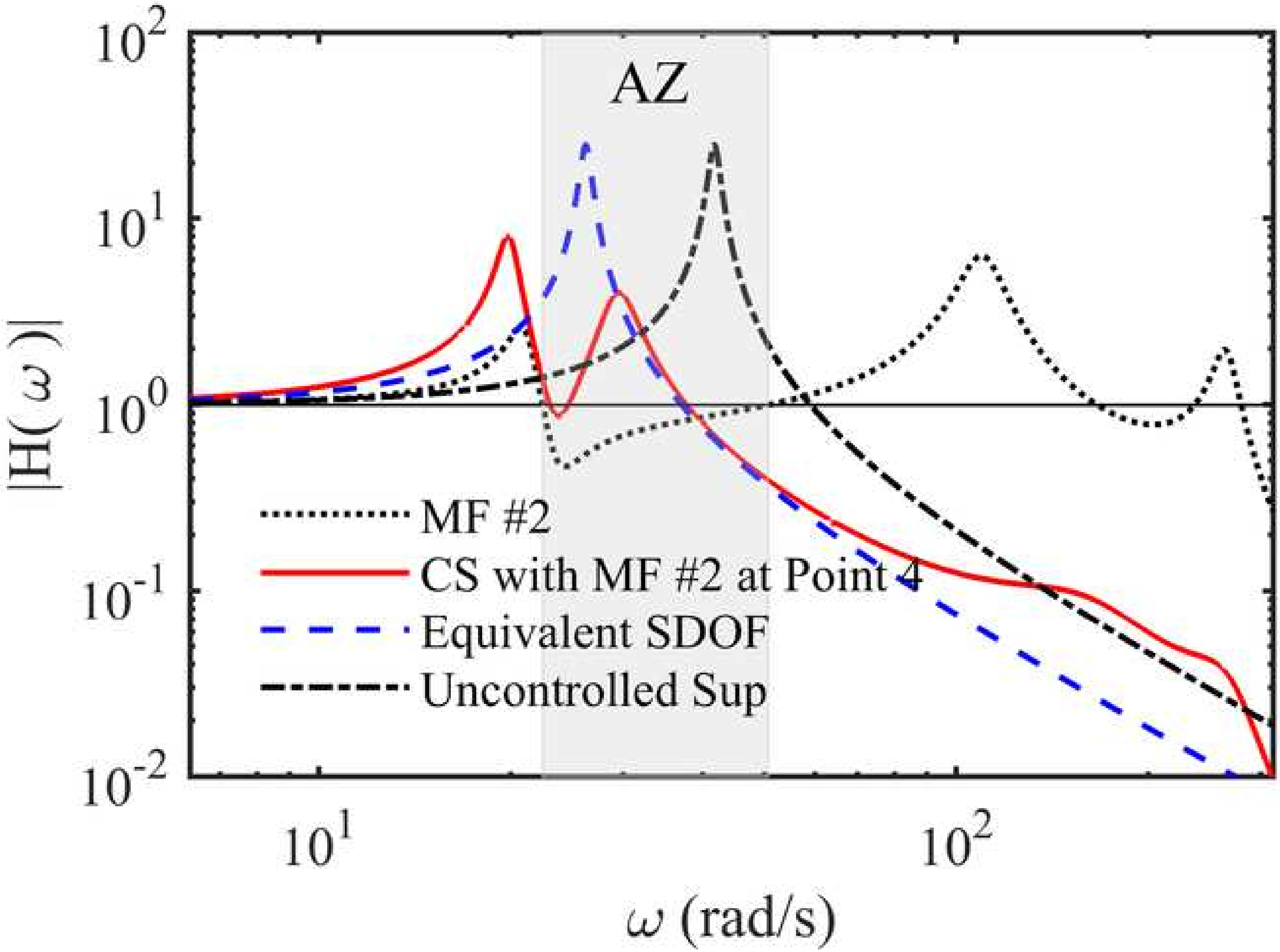
AZ
10^2
10^1
10^0
10^{-1}
10^{-2}
$|H(\omega)|$
10^1
10^2
ω (rad/s)
MF #2
CS with MF #2 at Point 4
Equivalent SDOF
Uncontrolled Sup

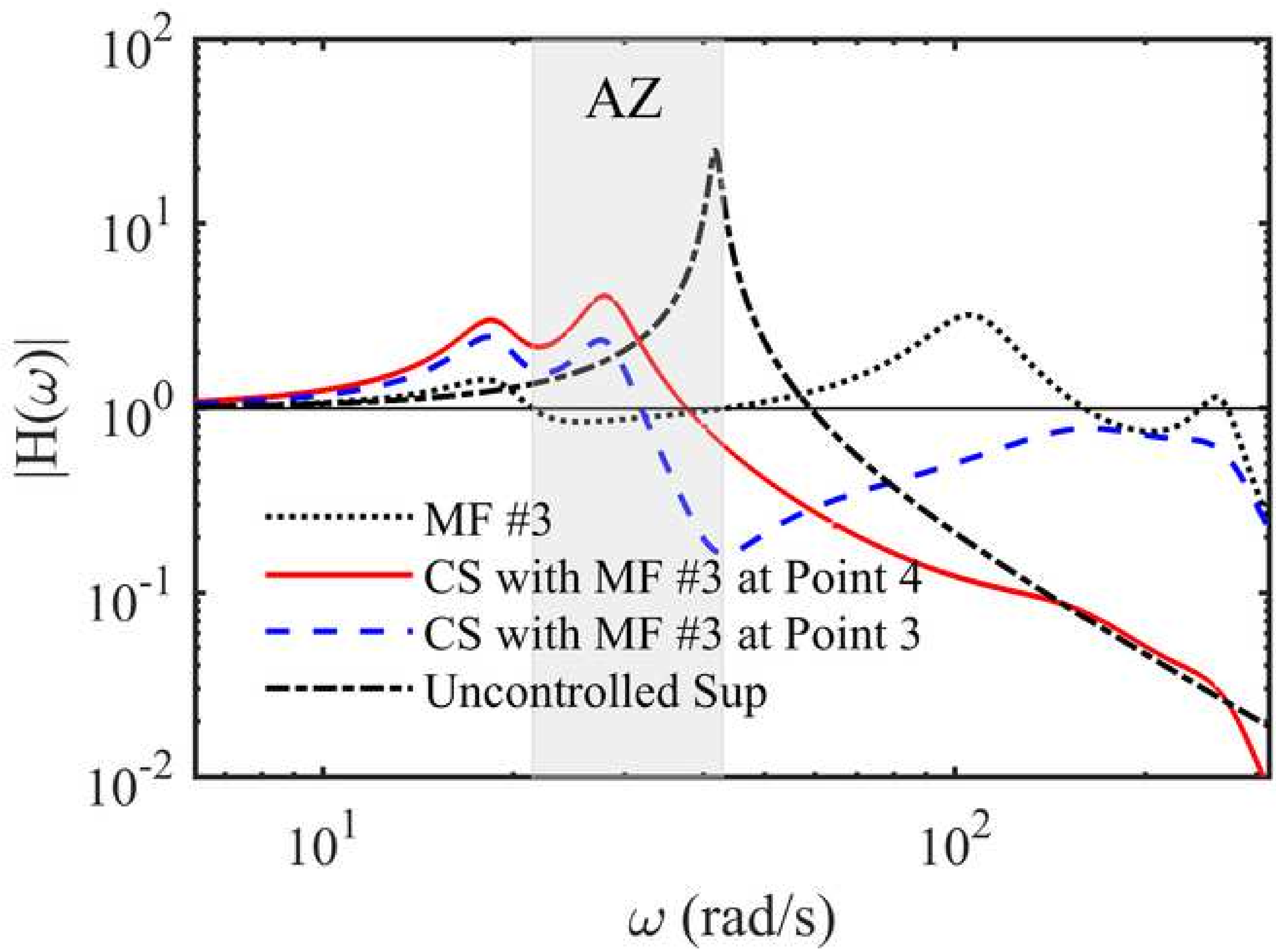
AZ
MF #3
CS with MF #3 at Point 4
CS with MF #3 at Point 3
Uncontrolled Sup
10^{2}
10^{1}
10^{0}
10^{-1}
10^{-2}
$|H(\omega)|$
10^{1}
10^{2}
ω (rad/s)

Figure list

Fig. 1 Uncoupled -System #1 and System #2- and coupled -System #3- systems composed of metafoundations (MF #1-#3) and superstructures.

Fig. 2 Liquid-filled tank system modelled by a set of generalized single-degree-of - freedom systems after Malhotra et al. (2000)

Fig. 3 Response spectra of the selected accelerograms with mean and uniform hazard spectra for OBE events

Fig. 4 Moduli of transfer functions $\left|H_{4,j}(\omega)\right|$ of coupled systems (CS) with optimized MF #1-#3 and that of the uncontrolled superstructure.

Fig. 5 The power spectrum density function (PSD) at the top of the metafoundation MF #1 $S_{P1}(\omega)$ and that at the base of MF #1 $S_{\ddot{x}_g}(\omega)$

Fig. 6 Transfer function moduli of MF #1 and contributions from different modes

Fig. 7 Linear correlation between the ratio of the standard deviation γ_{σ} and that of that peak response γ_{Resp} based on the seismic records listed in Table 2.

Fig. 8 Response contributions of non-attenuation (NAZ) and attenuation zones (AZ)

Fig. 9 Transfer function moduli of MF #1, coupled system (CS) with MF #1 and uncontrolled superstructure

Fig. 10 Transfer functions moduli of MF #2, coupled system (CS) with MF #2, the equivalent SDOF superstructure and the uncontrolled superstructure

Fig. 11 Transfer function moduli of MF #3, coupled system (CS) with MF #3 at Point 4, CS with MF #3 at Point 3 and the uncontrolled superstructure

ASCE Authorship, Originality, and Copyright Transfer Agreement

Publication Title: Journal of Engineering Mechanics

Manuscript Title/Number: EMENG-5178

Author(s) – **Names, postal addresses, and e-mail addresses of all authors**

Lei Xiao;Tongji University, 1239 Siping Road, Shanghai, China;1410213@tongji.edu.cn

Feifei Sun;Tongji University, 1239 Siping Road, Shanghai 200092, China;ffsun@tongji.edu.cn

Oreste Salvatore Bursi;University of Trento, Via Mesiano, 77, 38123 Trento, Italy;Oreste.Bursi@unitn.it

I. Authorship Responsibility

To protect the integrity of authorship, only people who have significantly contributed to the research or project and manuscript preparation shall be listed as coauthors. The corresponding author attests to the fact that anyone named as a coauthor has seen the final version of the manuscript and has agreed to its submission for publication. Deceased persons who meet the criteria for coauthorship shall be included, with a footnote reporting date of death. No fictitious name shall be given as an author or coauthor. An author who submits a manuscript for publication accepts responsibility for having properly included all, and only, qualified coauthors.

II. Originality of Content

ASCE respects the copyright ownership of other publishers. ASCE requires authors to obtain permission from the copyright holder to reproduce any material that (1) they did not create themselves and/or (2) has been previously published, to include the authors' own work for which copyright was transferred to an entity other than ASCE. For any figures, tables, or text blocks exceeding 100 words from a journal article or 500 words from a book, written permission from the copyright holder must be obtained and supplied with the submission. Each author has a responsibility to identify materials that require permission by including a citation in the figure or table caption or in extracted text.

More information can be found in the guide "Publishing in ASCE Journals: Manuscript Submission and Revision Requirements" (http://ascelibrary.org/doi/pdf/10.1061/9780784479018.ch05). Regardless of acceptance, no manuscript or part of a manuscript will be published by ASCE without proper verification of all necessary permissions to re-use. ASCE accepts no responsibility for verifying permissions provided by the author. Any breach of copyright will result in retraction of the published manuscript.

III. Copyright Transfer

ASCE requires that authors or their agents assign copyright to ASCE for all original content published by ASCE. The author(s) warrant(s) that the above-cited manuscript is the original work of the author(s) and has never been published in its present form.

The undersigned, with the consent of all authors, hereby transfers, to the extent that there is copyright to be transferred, the exclusive copyright interest in the above-cited manuscript (subsequently called the "work") in this and all subsequent editions of the work (to include closures and errata), and in derivatives, translations, or ancillaries, in English and in foreign translations, in all formats and media of expression now known or later developed, including electronic, to the American Society of Civil Engineers subject to the following:

- The undersigned author and all coauthors retain the right to revise, adapt, prepare derivative works, present orally, or distribute the work, provided that all such use is for the personal noncommercial benefit of the author(s) and is consistent with any prior contractual agreement between the undersigned and/or coauthors and their employer(s).
- No proprietary right other than copyright is claimed by ASCE.
- This agreement will be rendered null and void if (1) the manuscript is not accepted for publication by ASCE, (2) is withdrawn by the author prior to publication (online or in print), (3) ASCE Open Access is purchased by the author.
- Authors may post a PDF of the ASCE-published version of their work on their employers' ***Intranet*** with password protection. The following statement must appear with the work: "This material may be downloaded for personal use only. Any other use requires prior permission of the American Society of Civil Engineers."
- Authors may post the ***final draft*** of their work on open, unrestricted Internet sites or deposit it in an institutional repository when the draft contains a link to the published version at www.ascelibrary.org. "Final draft" means the version submitted to ASCE after peer review and prior to copyediting or other ASCE production activities; it does not include the copyedited version, the page proof, a PDF, or full-text HTML of the published version.

Exceptions to the Copyright Transfer policy exist in the following circumstances. Check the appropriate box below to indicate whether you are claiming an exception:

☐ **U.S. GOVERNMENT EMPLOYEES:** Work prepared by U.S. Government employees in their official capacities is not subject to copyright in the United States. Such authors must place their work in the public domain, meaning that it can be freely copied, republished, or redistributed. In order for the work to be placed in the public domain, ALL AUTHORS must be official U.S. Government employees. If at least one author is not a U.S. Government employee, copyright must be transferred to ASCE by that author.

☐ **CROWN GOVERNMENT COPYRIGHT:** Whereby a work is prepared by officers of the Crown Government in their official capacities, the Crown Government reserves its own copyright under national law. If ALL AUTHORS on the manuscript are Crown Government employees, copyright cannot be transferred to ASCE; however, ASCE is given the following nonexclusive rights: (1) to use, print, and/or publish in any language and any format, print and electronic, the above-mentioned work or any part thereof, provided that the name of the author and the Crown Government affiliation is clearly indicated; (2) to grant the same rights to others to print or publish the work; and (3) to collect royalty fees. ALL AUTHORS must be official Crown Government employees in order to claim this exemption in its entirety. If at least one author is not a Crown Government employee, copyright must be transferred to ASCE by that author.

☐ **WORK-FOR-HIRE:** Privately employed authors who have prepared works in their official capacity as employees must also transfer copyright to ASCE; however, their employer retains the rights to revise, adapt, prepare derivative works, publish, reprint, reproduce, and distribute the work provided that such use is for the promotion of its business enterprise and does not imply the endorsement of ASCE. In this instance, an authorized agent from the authors' employer must sign the form below.

☐ **U.S. GOVERNMENT CONTRACTORS:** Work prepared by authors under a contract for the U.S. Government (e.g., U.S. Government labs) may or may not be subject to copyright transfer. Authors must refer to their contractor agreement. For works that qualify as U.S. Government works by a contractor, ASCE acknowledges that the U.S. Government retains a nonexclusive, paid-up, irrevocable, worldwide license to publish or reproduce this work for U.S. Government purposes only. This policy DOES NOT apply to work created with U.S. Government grants.

I, the corresponding author, confirm that the authors listed on the manuscript are aware of their authorship status and qualify to be authors on the manuscript according to the guidelines above.

I, the corresponding author, confirm that the content, figures (drawings, charts, photographs, etc.), and tables in the submitted work are either original work created by the authors listed on the manuscript or work for which permission to re-use has been obtained from the creator.

I, the corresponding author, acting with consent of all authors listed on the manuscript, hereby transfer copyright or claim exemption to transfer copyright of the work as indicated above to the American Society of Civil Engineers.

Feifei Sun
Print Name of Author or Agent

Feifei Sun
Signature of Author of Agent

2019.11.4.
Date

NOTE: If you do not wish to sign the form digitally, please print, sign, scan, and email (books) or upload (journals) the form. More information regarding the policies of ASCE can be found in Publishing in ASCE Journals at https://doi.org/10.1061/9780784479018

Low-frequency and time-history analysis of one-dimensional uncoupled and coupled systems with optimal metafoundations

Vibration attenuations and amplifications of one-dimensional uncoupled and coupled systems with optimal metafoundations

Lei Xiao, Feifei Sun, Oreste Salvatore Bursi

Manuscript Number: EMENG-5178

The authors wish to thank the Reviewers for their comments and recommendations. The authors have addressed the Reviewers' comments as thoroughly as possible.

Below, the main comments of the reviewers are shown in black color. The authors' responses are given in *blue*. Major revisions suggested by the reviewers are clearly pointed out hereinafter and incorporated within the revised paper in red. Conversely, minor revisions are not explicitly shown here; however, they have been addressed accordingly in the revised manuscript.

Responses to Reviewer #1

Reviewer #1: In this article, Xiao et al. perform a numerical study on metafoundations and analyze their interaction with superstructures. With respect to their previous submission, the authors have shifted their attention to metafoundations, i.e., systems for which a spring-mass model represents a reasonable approximation. The article has been improved much with respect to the previous submission, and I think it could represent an interesting contribution to the seismic metamaterials community, since not many have analyzed the amplification effects of these systems at frequencies outside the attenuation zones. However, few issues still remain. First of all, the authors reference many times the work of Basone et al., using many of the procedures reported in that article. The authors should clarify that the present work is a follow-up on the other article and should specify with more clarity what the main contributions of the present work are. Also, some parts of the article can be written with more clarity. In conclusion, this article should be considered for publication in JEM upon revision.

In the following, the authors will find some detailed comments aimed at improving their manuscript.

Comment-1: This work seems to be a follow up on the article by Basone et al. The main novelty seems to be the analysis of the non-attenuation zones and of the amplification of the superstructure response due to the presence of the metafoundation. Is this correct? If so, I would make this more clear in the "Scope" section. Also, I would modify the title and mention something about the analysis of the vibration amplification phenomena in structures with metafoundations. Also, I would be explicit in the introduction and say that, "building from the work of Basone, the objective of this work is to [... adding a clear sentence about the main advancement of this work]"

The authors appreciate the revision work of Reviewer #1 and we agree with these suggestions. In the Scope Section, the following sentences are added to explicitly point this out.

“In order to shed light on both mechanisms and performance of MFs, especially the coupling effect of AZs and NAZs, this article proposes a phased approach which relies on the analysis of both uncoupled and coupled systems. More precisely, this research work is a continuation of the work by Basone et al. (Basone et al., 2018). Therefore, we start with the MF designed and optimized to control the response of a slender tank subjected to site-specific ground motion spectra, and we consider the main dynamic properties of the relevant superstructure.”

Moreover, the title is modified as follows:

“Vibration attenuations and amplifications of one-dimensional uncoupled and coupled systems with optimal metafoundations”

Comment-2: I would remove all abbreviations from the abstract (I don't think that is the right place to introduce abbreviations). Also, could the author try to limit them (PF, MF, AZ, NAZ, BI, OBE, UHS, CMS, SSE are way too many, in my opinion)? Otherwise, the reader is sometimes left searching the manuscript for the meaning of a certain abbreviation.

The authors agree with these suggestions. All the abbreviations in Abstract has been removed. Only ’MF’, ‘AZ’,’NAZ’, ‘OBE’ and ‘UHS’ remain in the revised version of the manuscript.

Comment-3: Some explanations are unclear. For example, please re-write the sentences on lines 100-105 and 145-153.

The sentences on lines 100-105 are revised as follows.

“Nonetheless, mitigation effects on the superstructure response are not explored in depth; in particular, they depend on base-isolation effects entailed by finite unit cells, the frequency range of AZs and resulting NAZs, indeed.”

The sentences on lines 145-153 are revised as follows.

“As stated in the Introduction, we consider two basic systems, named System #1 and System #3 in Fig. 1(a) and Fig. 1(c), respectively. Nonetheless, to take into account the shift of frequency of the original superstructure entailed by the flexibility of the outer frame of the MF, a new system called System #2 and depicted in Fig. 1(b) is considered. It is formed by replacing the original superstructure in System #1 with an equivalent SDOF structure, which reflects the first mode of the coupled superstructure-outer frame system. The MFs optimized in these three systems are denoted as MF #1, #2 and #3, respectively.”

Comment-4: The language can be improved. Not many typos are present but some sentences can be streamlined and made clearer.

Both grammar and language have been improved.

Comment-5: In Section "MFs performance in System #3" (please don't use abbreviations in section titles), the authors claim that MF3 causes a more favorable mitigation effect. Why is that the case? The authors could try to quantify this "favorability".

The title has been changed as “Performance of metafoundations in System #3”.

The performance of each metafoundation in the time domain is evaluated on the basis of the performance index γ_{Resp}, which defines the peak acceleration response ratio of the controlled and uncontrolled superstructure and is stated in Eq. 17. The statistics of γ_{Resp} are collected in Table 4. From that table, one can argue that both the mean value and the standard deviation of the coupled system with MF #3 are the lowest of the three coupled systems. The number of accelerograms in the case of MF #3, which would amplify the response of the controlled superstructure, is also minimal. All these figures indicate a more effective and stable mitigation effect of MF #3, compared with MF #1 and #2.

In the frequency domain, the moduli of transfer functions of superstructures in coupled systems with the three optimal MFs are compared in Fig. 4. MF #3 is the most effective in terms of amplitude reduction, which is consistent with the time domain results collected in Table 4.

The discussion about the performance evaluation stated in Section "Performance of optimized system" is revised as follows.

"With regard to the performance of the three MFs in the coupled system, the best mitigation effect is provided by MF #3, because MF #3 is directly optimized for the whole system. More precisely, as indicated in Table 4, a 23% average mitigation effect is achieved by MF #3 while that for MF #2 is 18% and MF #1 is ineffective in the average. The standard deviation of MF #3 is the lowest of the three MFs. The number of accelerograms that amplify the controlled superstructure response in the case of MF #3 is also minimal. All these figures indicate a more effective and stable mitigation effect of MF #3. Conversely, the mitigation effect of MF #1 is the worst. As far as the performance of MF #2 is concerned, this metafoundation, which is optimized in the uncoupled system but based on an equivalent SDOF, can achieve a performance close to that of MF #3.

With reference to the frequency domain, the moduli of transfer functions of superstructures $|H_{4,j}(\omega)|$ in coupled systems with the three optimal MFs are presented in ***Error! Reference source not found.****. Anew, MF #3 is the most effective in terms of amplitude reduction, as indicated by the transfer function amplitude of the superstructure with MF #3 $|H_{4,3}(\omega)|$; this is consistent with the results of Table 4. Conversely, only a limited benefit is achieved with MF #1. It is noteworthy to mention that both $|H_{4,2}(\omega)|$ and $|H_{4,3}(\omega)|$ exhibit two peaks due to the AZ caused by the inner resonators while $|H_{4,1}(\omega)|$ shows only a single peak entailed by the superstructure."*

Comment-6: In Table 4, why are there two columns with the same label?

The layout of this table is improved to make it clear. The second column refers to "Uncoupled System with MF #1"; the third column refers to "Coupled System with MF #1".

Comment-7: Figures 1 and 3 are redundant. Can the authors collapse figures 1, 2 and 3 in a single figure? Also, I am not sure that figure 4 is needed. Plus, this figure is unreadable unless the reader keeps looking back at Fig.3 to understand what those points 1, 2 and 4 are. Also, in order to be able to compare the behavior of MF1, MF2 and MF3, can the authors add the same reference (e.g. the uncontrolled superstructure response) to all plots? It would also be nice if the authors tried to use the same line markers for analogous quantities in those figures (e.g., the dashed blue line is the uncontrolled superstructure response in all figures).

The authors agree with these suggestions. Fig. 3 replaced Fig. 1. Fig. 4 has been removed. The FRF of the uncontrolled superstructure is added to all related figures, that is, Fig. 9-11 in the revised version. Legends are unified in those figures.

Comment-8: Fig.10 should be explained with more clarity. What does the yellow bar indicate, from a physical perspective? How can this bar be interpreted?

With regard to the new Fig. 8, the yellow bar defines the area ratio of the response PSD of the controlled and uncontrolled superstructures, as indicated below.

$$\gamma_A = \frac{\int_0^\infty S_{s1}(\omega)d\omega}{\int_0^\infty S_{UNC}(\omega)d\omega}$$

The standard deviation ratio γ_σ is defined as

$$\gamma_\sigma = \left(\frac{\sigma_a^{2,CON}}{\sigma_a^{2,UNC}}\right)^{0.5} = \left(\frac{\int_0^\infty S_{s1}(\omega)d\omega}{\int_0^\infty S_{UNC}(\omega)d\omega}\right)^{0.5} = (\gamma_A)^{0.5}$$

As indicated in the new Fig. 7, a high correlation between γ_σ and the response ratio of the controlled and uncontrolled superstructures γ_{Resp} is evident. Hence, in the previous version, we employed γ_A to estimate the response ratio of the controlled and uncontrolled superstructures γ_{Resp}. But for simplicity and clarity, we directly used γ_{Resp} instead of γ_A in the revised version.

The related part in Section " Quantification of non-attenuation zone and attenuation zone" is revised as follows.

"The corresponding results are depicted in **Error! Reference source not found.**, where the yellow bar defines the response ratio of the controlled and uncontrolled superstructures γ_{Resp}."

Comment-9: I am confused about the optimization procedure and I invite the authors to better explain it. Are the authors optimizing for maximum attenuation? Or are they optimizing for a combination of maximum attenuation in the AZ and lowest peaks outside of it? Just saying "we optimize for the variance ratio" is not clear enough.

More precisely, we optimized the maximum attenuation of the variance ratio, defined as

$$\gamma_{\sigma^2} = \sigma_a^{2,CON}(\boldsymbol{d})/\sigma_a^{2,UNC}(\boldsymbol{d})$$

where γ_{σ^2} is chosen as the objective function based on the reasons listed herein.

1) *γ_{σ^2} can be directly calculated in the frequency domain. Therefore, the existing soil models for power-spectrum density function evaluation, like the Kanai-Tajimi filter, can be used. By fitting the average power-spectrum density function of a set of selected accelerograms with the Kanai-Tajimi filter, construction sites can be taken into account. See, Basone et al., (2018). As a result, with respect to optimization procedures which consider peak*

responses of a set of accelerations in the time domain, the proposed optimization in the frequency domain is quite efficient.

2) *As shown in Fig. 7 of the manuscript, γ_{σ^2} and the peak response ratio γ_{Resp} are highly correlated. Hence, optimization results based on γ_{σ^2} can also attenuate peak responses to a large extent, as the average attenuation of peak responses shown in the last column of Table 4. A 23% average attenuation is achieved in the case of the coupled system with MF #3.*
3) *γ_{σ^2} is commonly used as the objective function in the optimization of passive structural vibration control, e.g. De Domenico and Ricciardi (2018).*

In the coupled system, it is not easy to find a performance index to measure the maximum attenuation in the AZ. In fact, the actual attenuation of the peak response is related to the frequency range of the AZ, the attenuation effect in the AZ, the amplification in the NAZ and the base-isolation effect.

As a result, the Section "Optimization procedure" of the manuscript is revised as follows.

"The autocovariance or variance of the superstructure absolute acceleration $\sigma_a^{2,CON}$ of each controlled system can be calculated by the Wiener–Khinchin theorem, as

$$\sigma_a^{2,CON} = E[a^2(\tau = 0)] = \int_0^\infty S_{si}(\omega)\, d\omega \;\; (i = 1, 2, 3) \qquad (14)$$

where $E[a^2(\tau = 0)]$ defines the expectation of the random variable a and τ is the time lag (Vanmarcke, 1976; Kjell, 2002). The variance of the uncontrolled superstructure can be obtained as

$$\sigma_a^{2,UNC} = \int_0^\infty |H_s(\omega)|^2 S_{\ddot{x}_g}(\omega)\, d\omega. \qquad (15)$$

Then, a variance ratio can be defined as

$$\gamma_{\sigma^2} = \sigma_a^{2,CON} / \sigma_a^{2,UNC} \qquad (16)$$

The variance ratio γ_{σ^2}, which is commonly used as the objective function in the optimization of passive structural vibration control, see among others (De Domenico and Ricciardi, (2018)), is selected as the objective function. By replacing $S_{\ddot{x}_g}(\omega)$ in Eq. (5), (6), (10) and (15) with the KC-fitted PSD for the OBE accelerograms obtained in the Section "Ground motion selection", an optimization in the frequency domain was carried out. As a result, in order to achieve the maximum attenuation of the variance ratio γ_{σ^2} based on the construction site, γ_{σ^2} was minimized in the frequency domain."

References

Basone F, Wenzel M, Bursi OS, et al. (2018) Finite locally resonant Metafoundations for the seismic protection of fuel storage tanks. Earthquake Engineering & Structural Dynamics.

De Domenico D and Ricciardi G. (2018) Optimal design and seismic performance of tuned mass damper inerter (TMDI) for structures with nonlinear base isolation systems. Earthquake Engineering & Structural Dynamics 47: 2539-2560.

Responses to Reviewer #2

Reviewer #2: The revised manuscript has several major modifications, especially in the model setup and the research method. By introducing the two uncoupled systems and comparing them with the coupled system, the coupling effects between the metafoundations (MFs) and the superstructure is better understood. Overall, the key concepts have been explained much better, and the methodology of the study makes more sense to me. However, there are still a few places where things should be clarified or explained to the reviewer's satisfaction.

Comment-1: In the rerevised manuscript, the transfer function Hx^{MF}, i.e., Eq. (2), is defined in a way that relates the relative displacement to the excitation (in the paper, x_g). However, equation (3) is valid for transfer functions defined with respect to the excitation acceleration, i.e., (x_g) ̈. The authors should double check the validity of equation (3). Moreover, the transfer function Hs (Eq. (4)) is obtained using a different definition other than the one used for Hx^{MF}. The definition of the transfer functions should be consistent throughout the paper. If the reviewer's argument is right, the authors should correct these equations as well as the remainder of the paper accordingly.

The authors appreciate the revision made by Reviewer #2.

We actually used the transfer function with respect to acceleration excitations instead of the one with respect to displacement excitations in the related Matlab codes. Both the text and Eq. (2) have been amended as follows.

"Given a harmonic acceleration excitation $\ddot{x}_g = e^{i\omega t}$ where $i = \sqrt{-1}$, the transfer function that relates the relative displacement of the system to the excitation can be expressed as

$$\boldsymbol{H}_x^{\boldsymbol{MF}}(\omega) = \frac{\boldsymbol{M}^{\boldsymbol{MF}}\boldsymbol{r}^{\boldsymbol{MF}}}{-\omega^2\boldsymbol{M}^{\boldsymbol{MF}} + i\omega\boldsymbol{C}^{\boldsymbol{MF}} + \boldsymbol{K}^{\boldsymbol{MF}}} \qquad (1)$$

"

The transfer function of the SDOF system, Eq. (4), is rewritten to be consistent with the case of a MDOF system as

"

$$H_s(\omega) = \frac{m^s}{-\omega^2 m^s + i\omega c^s + k^s} \qquad (4)$$

in which m^s, k^s and c^s are the mass, stiffness and damping coefficient of the superstructure, respectively."

Comment-2: For system 2, the one with the equivalent SDOF structure, its PSD is given in Eq. (6) with H_{eq} buried in the expression. The authors should provide the explicit formula of H_{eq} and guide readers how to get it.

The transfer function of the equivalent SDOF structure is the same of the transfer function of an SDOF structure except that the parameters of the equivalent SDOF structure are used. The *manuscript is revised to explicitly guide how to obtain parameters of the equivalent SDOF structure.*

"As far as System #2 is concerned, see Fig. 1b, we recall that the main characteristics of the coupled system of the original superstructure and the outer frame of the MF are dynamically represented by an equivalent SDOF system. The mass, eigenfrequency and damping ratio of the equivalent SDOF system are the corresponding parameters of the first mode of the coupled superstructure-outer frame system. As a result, the response PSD of the equivalent SDOF structure $S_{s2}(\omega)$ can be evaluated as

$$S_{s2}(\omega) = \left|H_{eq}(\omega)\right|^2 |H_1(\omega)|^2 S_{\ddot{x}_g}(\omega) \quad (6)$$

where $H_{eq}(\omega)$ defines the transfer function of the equivalent SDOF structure. $H_{eq}(\omega)$ can be easily obtained by substituting the parameters of the equivalent SDOF structure into Eq. (4)."

Comment-3: In Eq. (5) and (6), H_{MF} should be replaced by H_{MF1}.

Eq. (5) and (6) have been revised accordingly.

$$S_{s1}(\omega) = |H_s(\omega)|^2 |H_{MF1}(\omega)|^2 S_{\ddot{x}_g}(\omega) = |H_s(\omega)|^2 S_{P1}(\omega) \quad (5)$$

$$S_{s2}(\omega) = \left|H_{eq}(\omega)\right|^2 |H_{MF1}(\omega)|^2 S_{\ddot{x}_g}(\omega) \quad (6)$$

Comment-4: In the optimization procedure, the authors choose γ_{σ^2} as the objective function. However, they didn't give any explanations or citations why they made this choice. From the reviewer's standpoint, since this study has focused on the amplification in the non-attenuation zone (NAZ), the optimization should aim at evaluating the set of parameters which gives the minimum amplification effect in NAZ.

Thank you for your suggestions.

γ_{σ^2} is chosen as the objective function based on the reasons below.

1) *γ_{σ^2} can be directly calculated in the frequency domain. Therefore, the existing soil models for power-spectrum density function evaluation, like the Kanai-Tajimi filter, can be used. By fitting the average power-spectrum density function of a set of selected accelerograms with the Kanai-Tajimi filter, construction sites can be taken into account. See, Basone et al., (2018). As a result, with respect to optimization procedures which consider peak responses of a set of accelerations in the time domain, the proposed optimization in the frequency domain is quite effective.*
2) *As shown in Fig. 7 of the manuscript, γ_{σ^2} and the peak response attenuation ratio γ_{Resp} are highly correlated. Hence, optimization results based on γ_{σ^2} can also attenuate peak responses to a large extent, as the average attenuation of peak responses shown in the first column of Table 4. A 23% average attenuation is achieved in the case of the coupled system with MF #3.*

3) γ_{σ^2} *is commonly used as the objective function in the optimization of passive structural vibration control, e.g. De Domenico and Ricciardi (2018).*

We believe that a measure of the minimum amplification effect in NAZ can be represented by the amplitude of the transfer function of the superstructure. The optimization based on the maximum attenuation of the amplitude of the transfer function can achieve an optimal result. However, the use of γ_{σ^2} *as objective function allows for considering the construction site, as stated in point 1 above.*

The Section Optimization procedure is revised to clearly point out the reason behind the choice of γ_{σ^2} *as objective function.*

"The autocovariance or variance of the superstructure absolute acceleration $\sigma_a^{2,CON}$ *of each system can be calculated by the Wiener–Khinchin theorem, as*

$$\sigma_a^{2,CON} = E[a^2(\tau = 0)] = \int_0^{\infty} S_{si}(\omega)\, d\omega \;\; (i = 1, 2, 3) \qquad (14)$$

where $E[a^2(\tau = 0)]$ *defines the expectation of the random variable* a *and* τ *is the time lag (Vanmarcke, 1976; Kjell, 2002). The variance of the uncontrolled superstructure can be obtained as*

$$\sigma_a^{2,UNC} = \int_0^{\infty} |H_s(\omega)|^2 S_{\ddot{x}_g}(\omega)\, d\omega. \qquad (15)$$

Then, a variance ratio can defined as

$$\gamma_{\sigma^2} = \sigma_a^{2,CON} / \sigma_a^{2,UNC} \qquad (16)$$

The variance ratio γ_{σ^2}*, which is commonly used as the objective function in the optimization of passive structural vibration control, see among others (De Domenico and Ricciardi, (2018)), is selected as the objective function. By replacing* $S_{\ddot{x}_g}(\omega)$ *in Eq. (5), (6), (10) and (15) with the KC-fitted PSD for the OBE accelerograms obtained in the Section "Ground motion selection", an optimization in the frequency domain was carried out. As a result, in order to achieve the maximum attenuation of the variance ratio* γ_{σ^2} *based on the construction site,* γ_{σ^2} *was mini ized in the frequency domain."*

Comment-5: The following sentence starting from line 339 needs to be clarified: "In fact, this shift hindered the mitigation of the superstructure response of the coupled system #3 with MF #1."

This sentence means that due to the frequency shift of the superstructure, MF #1 fails to mitigate the response of the superstructure in the coupled system. The whole paragraph that starts in line 349 and provides reasons has been amended.

"The mitigation performance of MFs can benefit from the use of a flexible unit cell –flexible outer frame- which entails an isolation effect due to a superstructure frequency shift.

However, this shift hindered the mitigation performance of MF #1 in the coupled system. More precisely, MF #1 has been optimized in the uncoupled system. Therefore, it realizes an AZ which covers the eigenfrequency of the uncontrolled superstructure (dashed line), marked with a shaded area in Fig. 9. Nonetheless, when MF #1 is involved in the coupled system, due to coupling, the eigenfrequency of the superstructure shifts to a lower frequency value which results to be outside the AZ of MF #1. See, in this respect, the continuous line of the coupled system (CS) with MF #1. As a result, MF #1 fails to mitigate the seismic response of the superstructure in the coupled system."

Comment-6: In the section of "Frequency shift of superstructure", the authors mention that MF #1 and #2 are "designed" while MF #3 is "optimized" to exhibit certain features. Is there any difference between the design and optimization procedures? Is the optimization adopted in this section different from the previous one? The authors should specify and clarify how they design and optimize the MFs.

There is no difference in the optimization process. MF #1, MF #2 and MF #3 are optimized with the same procedure stated in Section "Optimization procedure" and the same objective function stated in Eq. (16). The only difference is that MF #1 and MF #2 are optimized in the uncoupled system while MF #3 is optimized in the coupled system.

As a result, Section "Frequency shift of superstructure" is amended as follows.

"The mitigation performance of MFs can benefit from the use of a flexible unit cell –flexible outer frame- which entails an isolation effect due to a superstructure frequency shift. However, this shift hindered the mitigation performance of MF #1 in the coupled system. More precisely, MF #1 has been optimized in the uncoupled system. Therefore, it realizes an AZ which covers the eigenfrequency of the uncontrolled superstructure (dashed line), marked with a shaded area in Fig. 9. Nonetheless, when MF #1 is involved in the coupled system, due to coupling, the eigenfrequency of the superstructure shifts to a lower frequency value which results to be outside the AZ of MF #1. See, in this respect, the continuous line of the coupled system with MF #1. As a result, MF #1 fails to mitigate the seismic response of the superstructure in the coupled system.

MF #2 depicted in Fig. 1(b) is also optimized in the uncoupled system. However, in order to take into account the aforementioned frequency shift, instead of the original superstructure an equivalent SDOF system is used. Therefore, MF #2 exhibits an AZ that covers the eigenfrequency component of the equivalent SDOF, as shown in Fig. 10. As a result, the peak frequency of the superstructure in the coupled system with MF #2, see the second peak of the continuous line of the coupled system with MF #2 in Fig. 10, actually falls into the AZ. Therefore, a more favorable mitigation effect is achieved with MF #2, w.r.t. the previous coupled system with MF #1."

References

De Domenico D and Ricciardi G. (2018) Optimal design and seismic performance of tuned mass damper inerter (TMDI) for structures with nonlinear base isolation systems. Earthquake Engineering & Structural Dynamics 47: 2539-2560.